I give permission for public access to my thesis and for copying to be done at the discretion of the archives' librarian and/or the College library.

_____*Anna Baccei*_____ _____*May 16th, 2011*____

Signature Date

Imaging the Cytoskeleton of Migratory Cells

By

Anna E. Baccei

A Paper Presented to the

Faculty of Mount Holyoke College in

Partial Fulfillment of the Requirements for

the Degree of Bachelor of Arts with

Honor.

Department of Biological Sciences

South Hadley, MA 01075

December 2010

This paper was prepared

under the direction of

Professor Rachel Fink

for eight credits.

This thesis is dedicated to Ms. Maureen Dugan, my tenth-grade AP biology teacher, who guided my love of science. It is also dedicated to my mother, Linda Baccei, who raised me in her lab. She is my biggest fan and my favorite scientist.

ACKNOWLEDGEMENTS

I honor and acknowledge my thesis advisor, Rachel Fink, and my second project advisor, Marian Rice. Rachel's wisdom and insight guided me both in the lab and in my writing, and her encouragement meant a great deal to me. She was as enthusiastic about my project as I was! Without Marian's constant assistance and dedication, my research would never have gotten off the ground. She was always there when I needed her, and I am extremely grateful for all her help.

I would also like to thank other members of the biology department, particularly – but not limited to – Sue Lancelle, Lamis Jarvinen, and Stan Rachootin. Sue, like Marian, was always willing to help, no matter how busy she was. I can't thank Lamis enough for the generous donation of her mouse stem cells as well as her support both in class and in the lab. I have to say a big "thank you" to my academic advisor Stan, who initially told me that he thought my project sounded like a good idea, and that I should go for it. His encouragement has been a big factor in shaping my science education at Mount Holyoke.

Nancy Lech and Eleanor Perrier in the Biology Office were always there to answer any questions I had; they never let the candy dish become empty, which was great on those long, marathon lab days when there was no time for lunch. I also thank Sharon Stranford for the use of her lab space to culture HeLa cells.

Others who have assisted me include Tatyana Svitkina of Upenn, who welcomed me into her office on a rainy day to chat about keratocyte extraction, and Omar Quintero, who generously allowed me to use the HeLa cells he left at Mount Holyoke. Omar has also been a mentor and a friend to me.

Finally, I am thankful for my friends and family, who have been understanding, patient, and always supportive.

TABLE OF CONTENTS

Anna E. Baccei

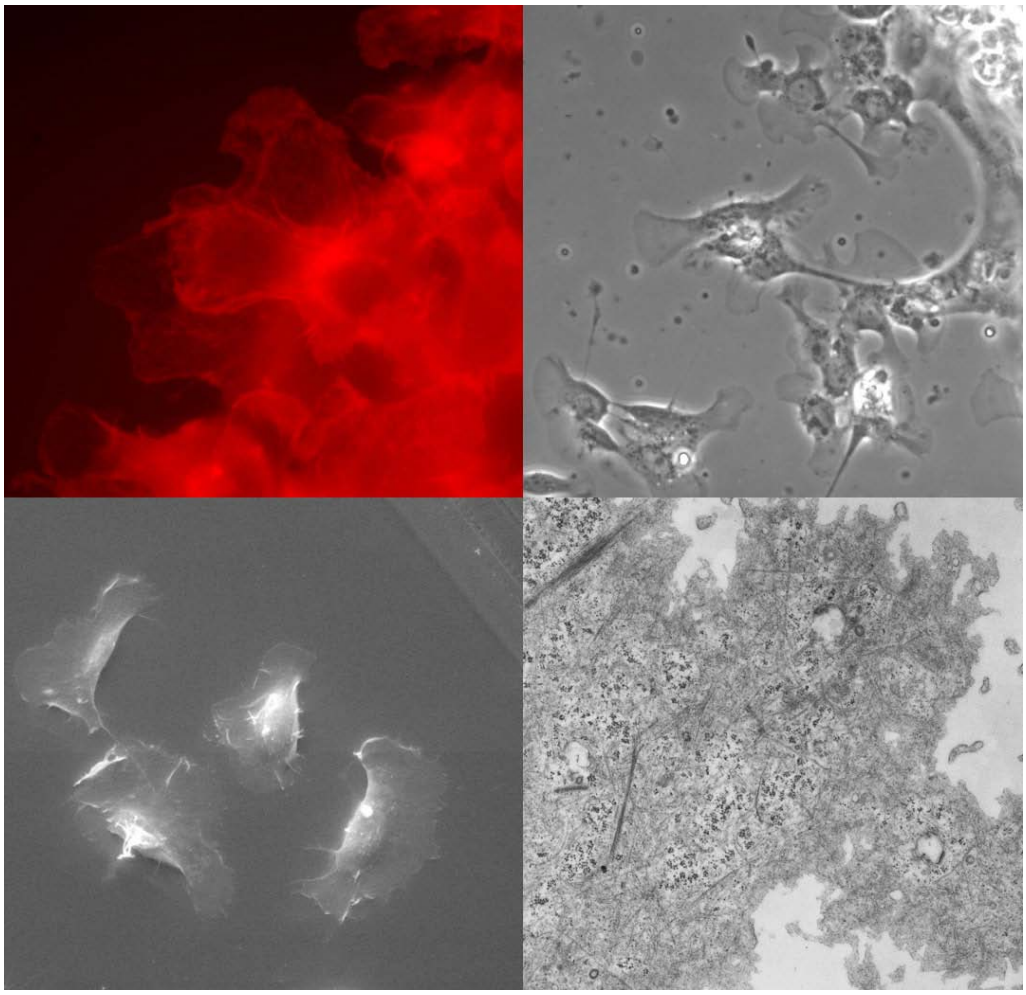

Imaging the Cytoskeleton of Migratory Cells

LIST OF FIGURES

PREFACE

Crawling cells are everywhere. They are in soil, skin, and bones; they digest pathogens and form scar tissue; they produce the material that is in hair and fingernails; and they form new blood vessels to bring nutrients to growing tissues – including tumors. Cells move alone, in clusters, or in sheets. During development, cells migrate to localize and specialize. Cell types that crawl include neurons, stem cells, fibroblasts, keratocytes, white blood cells, epithelial and endothelial cells, tumor cells, and free-living amoebae. They can migrate across the fibers of the extracellular matrix, through the extravascular space known as the stroma, and across glass coverslips, where they can be examined under microscopy.

Migratory cells have been a popular subject for imaging and micrography, the photography of objects under a microscope. Using glass lenses and photons – or magnets and electrons – microscopy reveals a world that is invisible to the naked eye. With equipment that is increasingly powerful, scientists can obtain images of objects no bigger than a few nanometers. Microscopes are nearly as diverse as the cells they magnify in terms of mechanics and the types of information they can produce. Compound light microscopy tells a different story from fluorescent microscopy, which in turn cannot completely match scanning or transmission electron microscopy. However, though the images are very different,

each is like a page in a book or a fragment in a stained glass window; by themselves they mean one or two things, but combined they present a rich and exquisite visual understanding of a complex process.

These bits of information reveal the world of migratory cells from a variety of aspects, but the points of crossover and the parallels between one type of image and another provide connections that unite individual micrographs into a mosaic of knowledge. This study is an investigation of five different motile cell types under five kinds of microscopy, with the goal of capturing images, making connections, and forming a general understanding of how cells crawl. Fish epidermal keratocytes, human cervical tumor cells, mouse bone-derived stem cells, mouse fibroblasts, and canine kidney epithelial cells are shown in the following pages under inverted culture microscopy, phase/contrast, fluorescence, scanning electron, and transmission electron microscopy.

Although the images reveal a great deal about cell motility, they also give feedback about the effectiveness of the methodology. Techniques involved with the preparation of cells for imaging, as well as microscopy protocols, determine the quality of the image – which in turn affects what can be learned. Therefore, this investigation is as concerned with the process as it is with the results. Published experiments can be compared, established protocols revised, and new steps added or modified in the laboratory to maximize the capabilities of the microscopes available.

This report begins with the mechanisms of crawling: cytoskeletal

structures, membrane dynamics, and cell-substrate interactions. It describes collective migration as well as independent migration, and gives some background as to why cells crawl in the first place. It also introduces the microscopy techniques and the cell types used in this study. Next, the experimental processes are described in detail, followed by the results. The discussion contains an evaluation of the significance of observed morphologies, applications of cell motility studies, and imaging technology. There is also a section dedicated to the promises, problems, and questions in the future of cell motility research. The major goal of this study is to explain and visually illuminate the process of imaging cells in motion, which itself is as intricate and dynamic as a migrating cell.

ABSTRACT

Cell migration is a complex and important process by which cells move along a surface or within a three-dimensional matrix. The mechanics of motility involve cytoskeletal rearrangement, membrane dynamics, and cell-substrate interactions. This investigation focuses on the morphologies, internal structures, and in vitro behavior of five migratory cell types using an array of microscopic techniques. Killifish keratocytes, HeLa cells, mouse bone-derived stem cells, mouse fibroblasts, and MDCK cells represent a diverse sampling of vertebrates and tissue sources; these cells were studied with brightfield, phase/contrast, fluorescence, and both scanning and transmission electron microscopy.

Keratocytes were plated on glass coverslips for phase/contrast time-lapse microscopy in order to create movies of migration. These cells, as well as HeLa cells, were also fixed with formaldehyde, extracted, and stained with a fluorophore that binds to actin in order to view the actin cytoskeleton. Keratocytes, HeLa cells, stem cells, and mouse fibroblasts were plated and fixed for scanning electron microscopy in order to examine external morphology and surface details. In one of these SEM experiments, the HeLa cells were extracted with detergent prior to fixation to remove the plasma membrane. Flat-embedded, thin-sectioned MDCK cells were imaged under transmission electron microscopy to reveal internal details at high magnifications.

The resulting images show both continuities and variability between the different cell types in this study. The results also highlight the importance of cellular imaging; both the process and the findings are applicable to cell motility research of all kinds, from in vitro studies to in vivo medical experiments. Ultimately, viewing the cytoskeleton and the larger structures it shapes helps elicit a conceptual understanding of cell migration.

INTRODUCTION

The ability of a cell to migrate along a substrate involves both intracellular forces and cell-environment interactions. Cell crawling plays a role in embryonic development, tissue growth and repair, and angiogenesis. Because tumor cells migrate when metastasizing, cell locomotion studies figure prominently in oncological research. Additionally, since many stem cells exhibit this property, a newly-emerging field focuses on understanding the mechanisms and circumstances of stem cell migration.

Cells migrating along a substrate exhibit characteristic movement often described by four steps **(Fig. 1)**: extension/protrusion, adhesion, contraction/translocation, and detachment (Mitchison and Cramer 1996). Seminal research leading to this model of cell migration was carried out by Michael Abercrombie in the 1970's (Bailly and Condeelis 2002), who found that these four steps occur simultaneously and continuously as the cell crawls (Abercrombie et al. 1970). The first step is the formation of motility structures that protrude outward from the main body of the cell, toward the intended direction of migration. Integrins and other adhesive proteins then anchor the front of the cell to the substrate, providing traction to enable the cytoplasm to stream forward. The original adhesion, now at the rear of the cell, then becomes severed via proteases and contractile forces (Ananthakrishnan and Ehrlicher 2007).

The structured protrusions cells use to crawl can be visualized under the microscope. These protrusions include lamellipodia and filopodia **(Fig. 2)**, whose number, size, and location on the cell body can convey a wealth of information such as cellular orientation. The front-most part of the cell, with respect to its

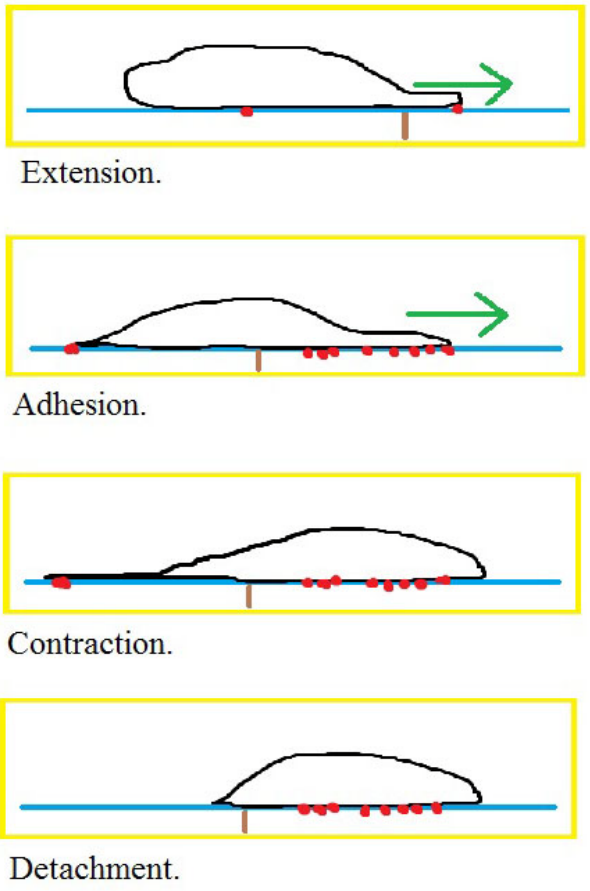

Figure 1. Diagram of actin-based cellular motility.

Actin polymerizes at the leading edge to form a protrusion in the forward direction, indicated by the green arrows, to initiate crawling. Focal adhesions (red) are formed between the base of the cell and the substrate to generate traction. Contraction of the cytoplasm moves the cell forward. Finally, focal adhesions at the rear of the cell are disassembled.

direction of movement, is known as the leading edge; this is where the leading lamellipodium or filopodium is found. Similarly, the portion furthest from the destination is the lagging or trailing edge.

Filopodia are long and slender, and sometimes have a direct role in locomotion – but they can also function as environmental sensors. Filopodia, like many other motility structures, are actin-based (Bray 2001, 25).

Lamellipodia are broad, semi-circular, shield-like formations. In some cells, the arc of a lamellipodium – at its largest – can dwarf the body of the cell. The leading edge of the lamellipodium is rich with branched actin filaments, which push the membrane forward at many contact points (Bray 2001, 123). "Ruffling," a phenomenon visible under time-lapse video microscopy, occurs at sites where actin microfilament cross-linking and reorganization occurs and pushes against the membrane. Under phase/contrast, ruffling is observed as dark, wave-like undulations originating at the very front edge of the lamellipodium and moving rear-ward toward the main cell body (Borm et al. 2005). A popular cell type for visualizing ruffling under time lapse is the keratocyte **(Movie 1)**. Lamellipodia, despite their large spreading area, are very flat: only 110-160 nm thick in fibroblasts (Abraham et al. 1999).

Figure 2. Filopodium and lamellipodium in HeLa cells migrating away from an area of high cellular concentration.

This image of fluorescent-stained actin in HeLa cells shows two kinds of cytoskeletal structures formed when a heavily seeded area of the coverslip is scraped off, creating a gap between the cells. A filopodium (A) and an emerging lamellipodium (B) are visible in this photograph. (C) shows a section of the empty area, where the tip of a scalpel was used to scratch a straight line across the coverslip. The cells along the scalpel's path necrosed and floated away, leaving the area of unoccupied coverslip seen here. Note the brightness of the fine filaments - arranged in a feathery structure - around the edge of the newly-forming lamellipodium. This indicates a high concentration of actin in this spot, where many branched microfilaments are constantly being polymerized at the leading edge so that the cell can crawl in that direction. Scale bar = 10 µm.

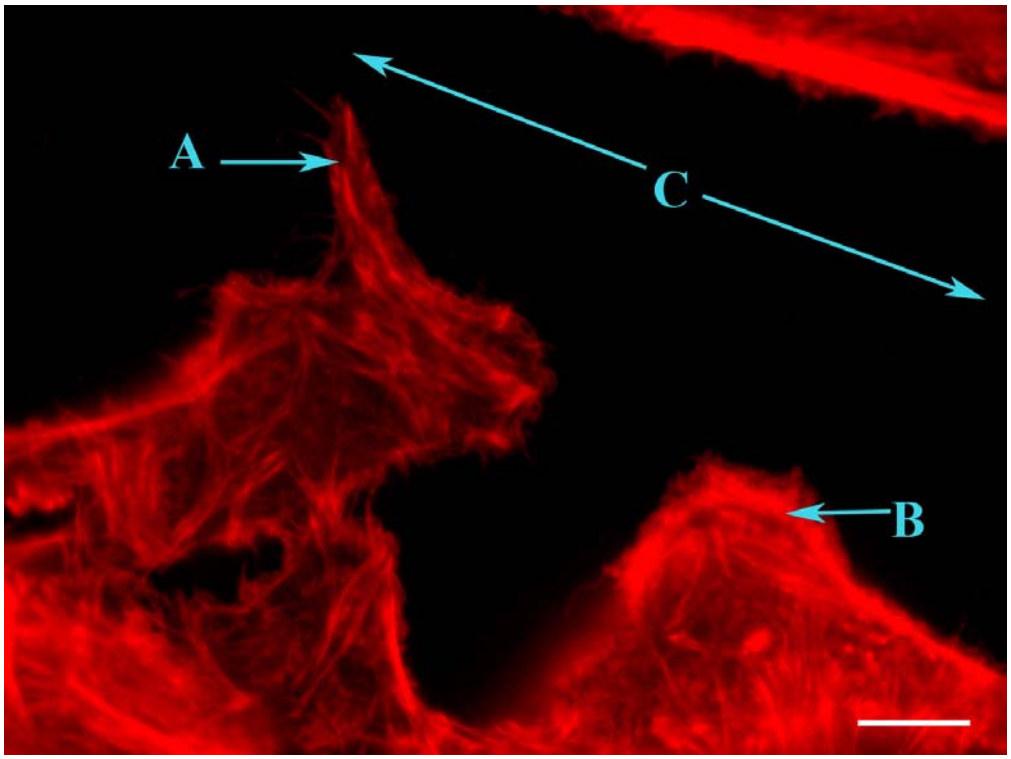
A
C
B

Another actin-based structure easily observed under certain types of microscopy is the stress fiber. Stress fibers **(Fig. 3)** are prominent, cross-linking, tension-bearing microfilament bundles found within the cytoskeletal network of the cell (O'Neill 2009). Actin polymerization in some intracellular stress fibers results from and begins at focal adhesion sites, while other stress fibers are not attached to focal adhesions. The latter, known as transverse arcs, are found parallel to the leading edge and are connected on both ends to dorsal stress fibers, which are associated on one end with focal adhesions. Ventral stress fibers are typically found more toward the rear of the cell, and are attached on both ends to focal adhesions (O'Neill 2009). There is tensile force between focal adhesions and the growing stress fibers associated with them (Alexandrova et al. 2008).

Finally, retraction fibers **(Fig. 4)** form at the tail end of the cell when a rear focal adhesion does not detach, causing the cell to elongate as the leading edge pulls the main cell body forward. Often these adhesions will rupture suddenly from the pulling force, which creates elastic tension; in such cases, the retraction fiber is quickly drawn forward into the main cell body. Sometimes the integrins are so tightly bound to the substrate that the cell actually breaks, leaving behind some of its material at the site of the focal adhesion (Bray 2001, 125-126). Retraction fibers, like leading edge protrusions, give clues as to the cell's directionality.

Figure 3. Stress fibers in a fluorescent HeLa cell stained for actin.

The thick, bright fibers indicated by the white arrows are likely to be ventral stress fibers. The blue arrow shows a transverse arc, which is parallel to the cell's leading edge and which links to several dorsal stress fibers (green arrows). Interestingly, the two cells in this image appear to have been migrating toward each other. Scale bar = 10 μm.

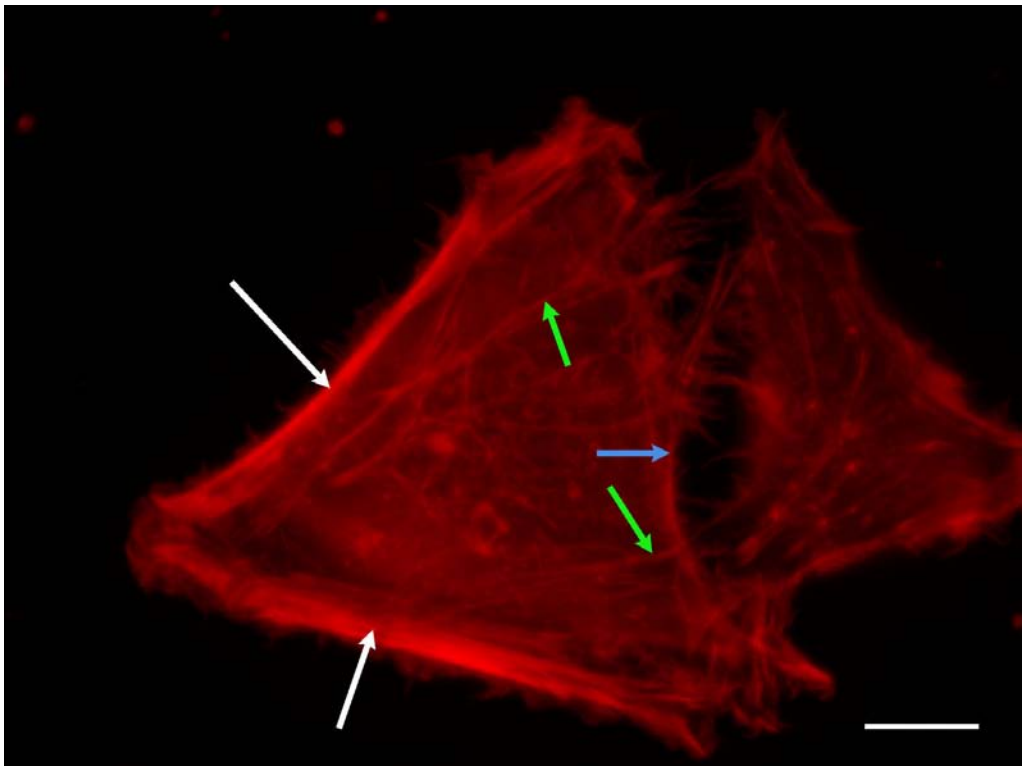

Figure 4. Retraction fiber observed in a keratocyte crawling away from a neighboring cell.

The green arrow indicates the direction of migration for the keratocyte in question. Its long retraction fiber (red arrow) extends nearly twice the length of the cell. There is another, smaller retraction fiber running parallel right beside it. Scale bar = 5 µm.

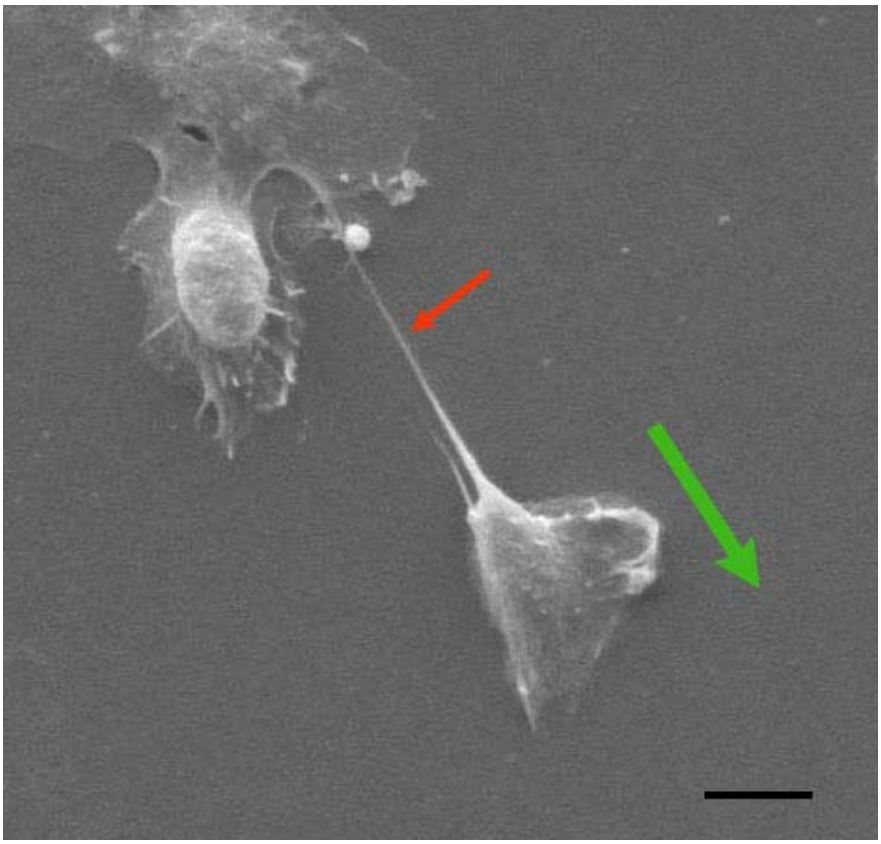

Filopodia are characterized by long, parallel arrays of microfilaments. This arrangement of straight bundles was thought to be necessary for maintaining physical pressure against the plasma membrane, facilitating forward momentum while preventing backtracking. However, studies involving both replica electron microscopy and fluorescence microscopy reveal that filopodia often exist even when the underlying microfilaments are arranged in less organized clusters, or more rarely, when there is no actin at all (Yang et al. 2009). Morphology-based studies are further complicated by the fact that filopodia can organize from actin filaments converging from lamellipodia (Yang et al. 2007). In brief, filopodia can reorganize into lamellipodia and vice-versa.

A different microfilament configuration occurs in lamellipodia. Here, the leading edge is much wider than it is long - exactly the opposite of a filopodium - and the actin microfilaments form a branching, criss-crossing network. Microfilaments close to the plasma membrane constantly shorten and lengthen as the cell advances; actin subunits depolymerize from the pointed end (more distal to the membrane) and are recycled forward to the barbed end, where the actin-binding protein profilin promotes polymerization. Nucleation of new filaments at the leading edge is facilitated by an actin-related protein complex (Arp 2/3), which nucleates branching at those sites (Goley and Welch 2006). **Figure 5** shows a model for the binding of Arp2/3 to a pre-existing actin filament, and the subsequent formation of a new branch. If a migrating cell is treated to remove its plasma membrane, the dense actin meshwork at the leading edge can

be visualized under the electron microscope **(Fig. 6)**.

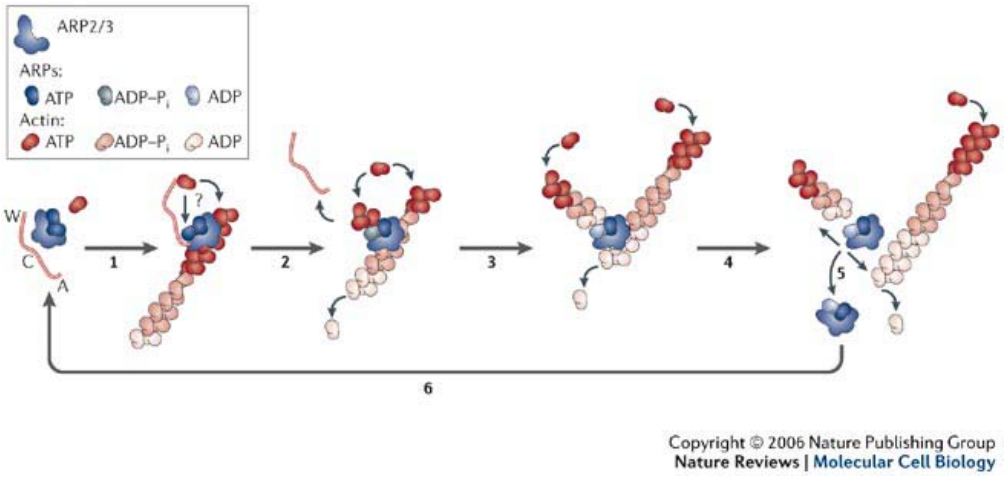

Figure 5. Model of Arp2/3-mediated microfilament nucleation.

In step 1, The Arp2/3 complex of proteins attaches to an existing microfilament and nucleates a new branch (Goley and Welch 2006). ATP-bound actin monomers polymerize onto the growing branches in steps 2 and 3. ATP is hydrolyzed into ADP as the microfilament ages; in steps 4 and 5, actin monomers and Arp2/3 proteins fall away to be recycled forward as the cell advances. Figure from Goley and Welch 2006.

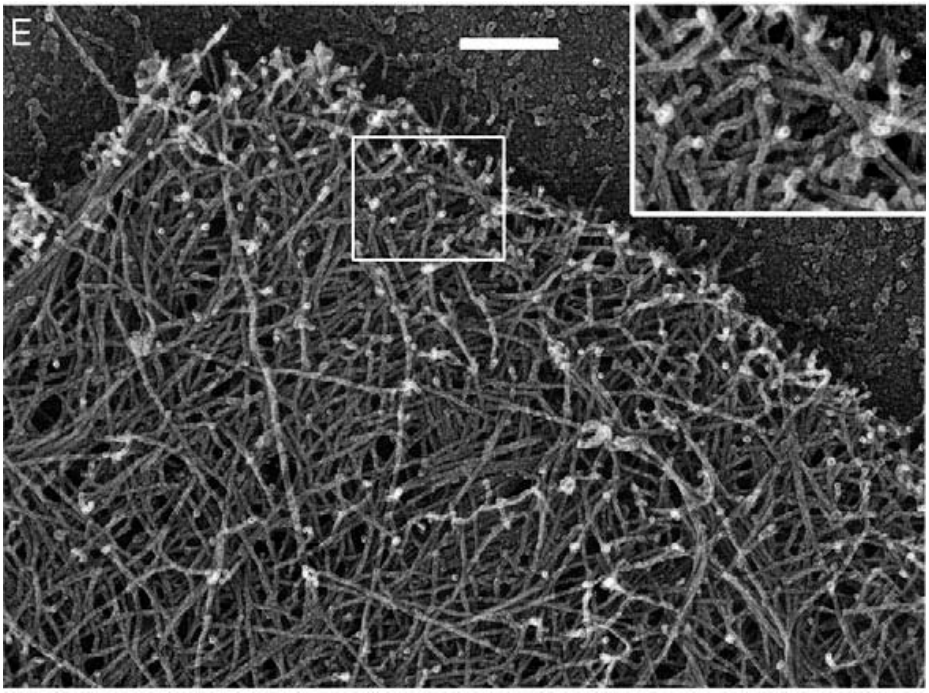

Figure 6. Replica EM of branched microfilaments at the leading edge (from Svitkina 2007).

This platinum replica EM micrograph, taken from Fig.2 of Dr. Tatyana Svitkina's 2007 publication in *Methods in Cell Biology*, shows the very front edge of a rat embryonic fibroblast with plasma membrane removed. The branched actin microfilaments are visible in amazing detail. Scale bar = 0.2 μm.

The phenomenon of retrograde flow of actin occurs constantly as depolymerized actin monomers and intact microfilaments are pushed backward, opposite to the direction of migration, due to the combined effects of polymerization at the leading edge and myosin motors (Ananthakrishnan and Ehrlicher 2007). The exact role of these myosins is still under active investigation. There is strong evidence for a biphasic relationship between the strength of

cell-substrate adhesion and retrograde flow; an intermediate threshold of adhesion-based traction forces is necessary for proper microfilament retraction and forward migration, above which the cell cannot contract and below which the cell cannot protrude (Alexandrova et al. 2008). Rapidly-moving cells – such as keratocytes – have high protrusion rates and low retrograde flow, while some slower cells – like fibroblasts – have simultaneously dense adhesions and low retrograde flow (Alexandrova et al. 2008).

Actin polymerization at the leading edge requires membrane flexibility. The thermodynamic properties of the plasma membrane allow Arp2/3 branched actin microfilaments to polymerize just inside the phospholipid bilayer as the membrane fluctuates, momentarily exposing just enough room to allow actin monomers to move in between the barbed end of the microfilament and the membrane. In this "ratchet model," elongating actin filaments create a pushing force against the plasma membrane that drives the cell forward (Theriot 2000). There is also evidence to suggest that endocytosed vesicles recycle membrane phospholipids to the leading edge from other parts of the cell. The insertion of these vesicles into the plasma membrane at the leading edge provides the membrane material for protrusion to occur (Casanova 2002).

Other lipids also play a key role in cell migration. Cholesterol affects plasma membrane microviscosity, which correlates with membrane softness or stiffness. Cholesterol saturation in the plasma membrane increases microviscosity, which means the membrane is stiffer, a change that is thought to promote the

response of increased actin polymerization (Vasanji et al. 2004). However, cholesterol oversaturation makes the membrane too stiff, decreasing actin polymerization (Theriot 2000).

Cells can move in groups as well as singly. In culture, epithelial and endothelial cells grow to confluence, packed tightly adjacent to one another in flat sheets called monolayers. They pass and receive signals from neighboring cells through cell-cell junctions (Sammak 1997). They migrate collectively and exhibit contact inhibition, an anti-tumor mechanism which prevents continued mitosis once confluence has been achieved (Seluanov 2009). These cells are stimulated to move into a wounded area by both the cessation of contact inhibition as well as paracrine signals given off by injured cells nearby as part of a wound-healing response. Mechanical breakage of cells also causes the release of intracellular signal molecules, which attract intact cells to the wound site (Sammak 1997). Tumor cells form monolayers, but unlike non-cancerous cells, they persist in proliferating regardless of contact with neighboring cells. New daughter cells must then overlap older cells that occupy the surface area of the substrate, forming layers upon layers of cells.

Mechanistically, intercellular coordination of collective migration is not extremely well-understood, though researchers take several angles when approaching this problem. One is simple cell-cell adhesion, where mechanical stress exerted on one cell by another may drive motility (Rørth 2009). However, there is strong experimental evidence that this pulling force would not be

sufficient, especially for large numbers of cells. Another idea is that focal adhesions of crawling cells change the properties of the substrate, altering stiffness, which in turn draws other cells in the same direction (Rørth 2009). In this model, mechanotransduction pathways enable cells to sense the stiffness of the substrate and respond by spreading and moving (Chowdhury et al. 2010). Despite the many similarities that are displayed by monolayer-forming cells, specific behaviors, growth rates, migration velocities, and coordination mechanisms vary between different cell types (Rørth 2009).

When analyzing the mechanisms and structures involved in cell locomotion, it is important to understand that – though random crawling is possible, especially in an artificial in vitro environment – cells move in response to environmental stimuli. Migratory cells receive information from their environment that triggers and directs their movement. The four main types of signals are chemotaxis, galvanotaxis (cell movement in response to an electrical field), haptotaxis, and contact guidance.

Chemotaxis is directional cell movement in response to a chemical signal, and involves recognition of a signal molecule by surface or transmembrane receptors. A well-studied example of chemotaxis is the aggregation of starved *Dictyostelium discoideum* amoebae, the unicellular life stage of this bacteriovorous cellular slime mold **(Fig. 7)**. In the 1940's Dr. J.T. Bonner of Princeton University studied and described the way individual amoebae plated on agar aggregate in a streaming fashion, eventually forming a colony of cells that

behave like a single, multicellular organism. His experiments eliminated other potential stimuli for directed migration, leading him to conclude that a diffusible chemical attractant - present in highest concentration at the epicenter of aggregation - induced the amoebae to migrate (Bonner 1947). The identification of cyclic AMP (cAMP) as the specific chemotactic molecule soon followed (Konijn et al. 1968).

Two other categories of directional cell motility involve a higher degree of cell-substrate interaction. Haptotaxis is migration in response to a concentration gradient either of chemicals bound to the substrate or of adhesive molecules in the substrate. Contact guidance relies on mechanosensory ability, where the tactile properties of the ECM are perceived by the cell (Lo et al. 2000). In such cases these physical interactions must be transduced into internal chemical signals that a) allow the cell to sense the nature of its location along the substrate and b) direct movement along the necessary path (Chowdhury et al. 2010). Mechanotransduction is a process that is not well understood, but intermembrane proteins involved in focal adhesions (i.e. the integrin family) are most likely involved.

Cells moving through a viscous microenvironment could not maintain motility without traction forces helping them grip the substrate. Focal adhesions are spots of concentrated cell-substrate attachments, mediated mainly by the class of transmembrane proteins known as integrins. The concentration and spatial

Figure 7. Streaming aggregates of *Dictyostelium discoideum* amoebae.

This image shows the pattern of migration of individual slime mold amoebae as they aggregate in response to starvation. Eventually the aggregate will condense to form a slug that looks and behaves like a true multicellular organism, migrating directionally before settling to form a fruiting body whose spore case will then break open to release thousands of amoebae – completing the life cycle of the cellular slime mold. It is now known that cAMP molecules are synthesized, given off, recognized, and recycled by amoebae during aggregation, attracting individual cells to one another and then to the crowded epicenter. This image was taken under 43x magnification.

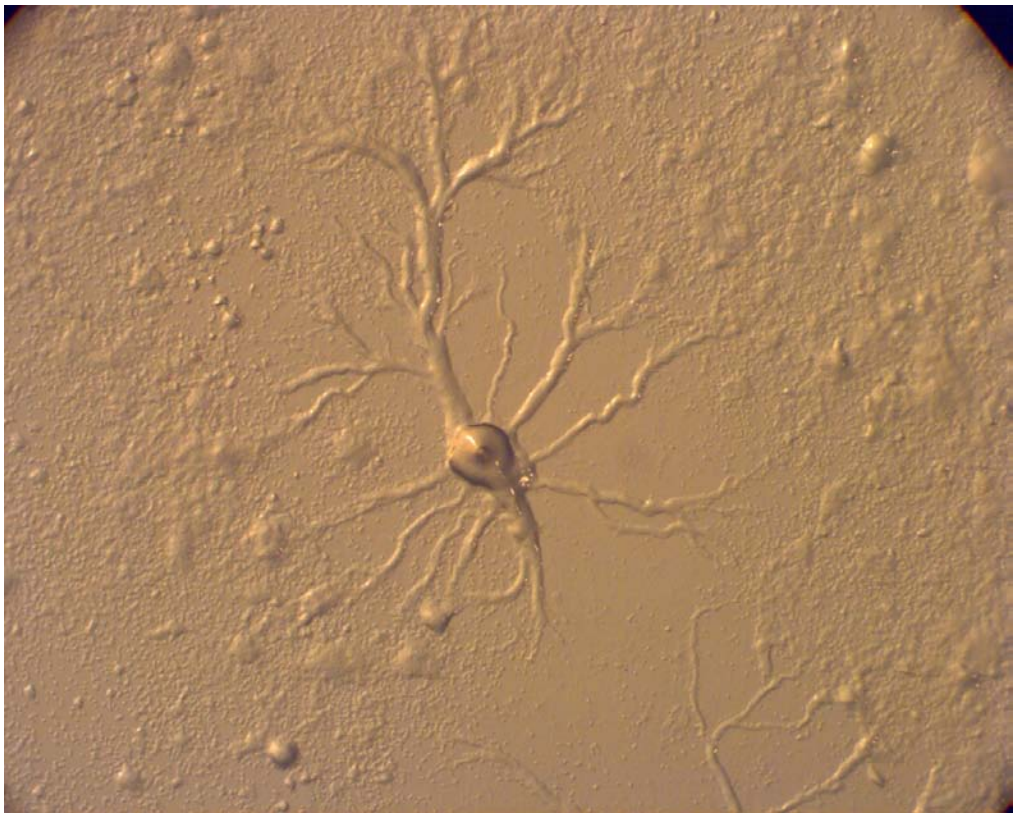

distribution of focal adhesions vary by cell type. Traction generated by these adhesions enables the cell to protrude forward while preventing it from slipping backward (Ananthakrishnan and Ehrlicher 2007).

Substrate rigidity or flexibility, which depends on the density and proportion of different extracellular materials, has an effect on cell softness or stiffness (as defined by the ratio of strain to stress) (Chowdhury et al. 2010). This in turn influences spreading ability and lamellipodia formation, which affects motility. Local stress applied against cells at the site of these adhesions influences the spreading area of the lamellipodia, particularly for inherently softer cells such as embryonic stem cells. Such data support the idea that cell softness or stiffness is altered in response to mechanical guiding forces in the substrate (Chowdhury et al. 2010). Migrating cells favor stiffer substrates, and can change direction, conformation, and motility rates upon encountering more flexible regions.

Microscopy of migratory cells

Imaging migrating cells is critical to their understanding. This study is concerned with analyzing, using, and sometimes revising current techniques in motile cell and cytoskeletal microscopy. From cell culture to final image, the laboratory procedures vary from cell type to cell type and from microscope to microscope. Additionally, each procedure differs in accordance with the form of desired information. A whole-cell surface image, for example, requires different preparation from an internal view of the cytoskeleton. Details of these preparations are described in the materials and methods section, but the main argument is that each form of microscopy - from the low-magnification dissecting microscope to the high-powered transmission electron microscope - provides information about the physical basis of cell motility from a slightly different angle. These pieces of information have parallels with one another, contrasts between one another, and cross-over points where they begin to tell the same story and then diverge. Analyzed together, these layers of understanding constructively support an overall picture of cell motility.

A starting point for imaging experiments involves viewing whole tissue samples or, in the case of tumor and stem cells, whole colony samples. The differences between the way each cell type in this study populates a culture flask or coverslip are striking. Stem cells grow in colony-forming units (CFUs), which originate from a single, clonal cell and enlarge outward via cell division and migration. Their ideal concentration is semiconfluent, such that they do not adjoin

neighboring cells (except sometimes through sensory filopodia), yet are seeded heavily enough to receive signals from nearby cells and colonies. Contrastingly, HeLa and MDCK cells are healthiest when they form a fully confluent monolayer of adjoining cells. *Fundulus* keratocytes, on the other hand, are difficult to isolate in sufficient quantities to cover the entire surface area of the coverslip. They start out as tightly adherent cells in clumps of scale tissue and then individual cells migrate away, remaining perfectly healthy when they are at a distance from other cells. The low concentration of keratocytes - except at the sites of tissue deposits - makes them difficult to see under the dissecting microscope because they do not form a film like the other cell types. The compound inverted culture microscope set at 100 or 400x is useful because it reveals the presence or absence of cells while they are still in the petri dish, either confirming that there are enough cells to proceed with the fixation or showing the opposite. Furthermore, dissecting and culture microscopes are useful for visualizing cells on plastic coverslips coated with poly-L-lysine, an artificial substrate that is useful for inducing cells to adhere and to crawl, but that otherwise impedes the precise passage of light necessary for compound microscopy.

Compound light microscopy is an extremely useful resource not only as a way to image cells and collect data, but also to finalize culture techniques and verify the presence and quality of cultured cells. It is also a good way to watch live cells in motion. Because live cells in culture media can survive on a glass slide, it is possible to watch them in real time as well as capture time-lapse videos

of their movement **(Movie 2)**.

Phase/contrast microscopy involves the use of a phase ring and annulus that condense light into two parallel rays, which variably diffract when they hit the sample in accordance with areas of higher or lower optical densities. This produces contrast in a sample that is fully or near transparent under brightfield, which involves only a single beam of light. **Figure 8** provides an example of phase/contrast microscopy of an MDCK cell.

In fluorescence microscopy, a sample stained with or expressing fluorophores emits light at frequencies determined by the absorption spectrum of the fluorophore. Electrons are excited to a higher valence shell by the absorption of light energy, and when they return to their original orbital position, they re-emit some of that energy in the form of colored light. Some energy is lost in the transfer, so emitted light is always at a lower frequency (longer wavelength) than absorbed light. Different filter packages, corresponding to different photon frequencies of the activating beam, are used for different fluorophores. Ultraviolet (UV) absorption causes emission in the blue spectrum, blue absorption causes emission in the green spectrum, and green absorption results in red emission. **Figure 9** shows examples of fluorescent staining observed under two different filters.

Scanning electron microscopy (SEM) involves the interaction of electrons – rather than photons – with the surface of a sample. The resolving power of electrons is much higher than the 200 nm resolution limit of photons. In a good

Figure 8. Phase-contrast image of a migrating MDCK cell.

This micrograph was taken during an experiment involving fluorescent staining. It shows the cell membrane (A), nucleus (B), lamellipodium (C), and various dense regions containing organelles. Phase-contrast micrographs are often taken for comparison purposes during fluorescent imaging, since excitation wavelengths used in fluorescence microscopy do not illuminate the sample, only the fluorophores embedded within it. Scale bar = 10 μm.

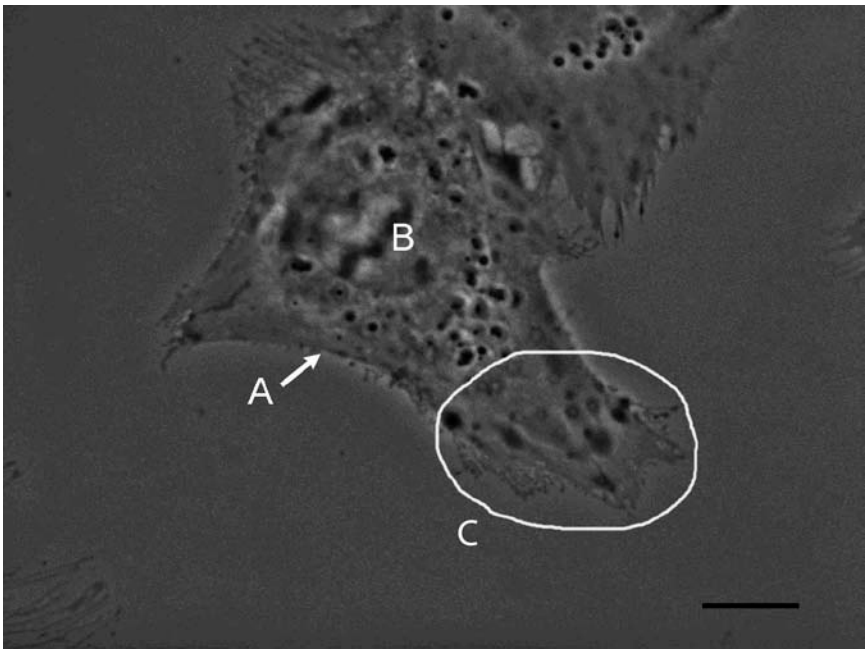
B
A
C

Figure 9. Examples of fluorescence microscopy.

The top panel shows mitochondria and endoplasmic reticulum of MDCK cells stained with DiOC6. The excitation wavelengths for this fluorophore are in the blue spectrum, so the sample glows green. On the bottom, MDCK nuclei are stained with DAPI, which is excited by UV wavelengths and emits blue light. Among the nuclei in this panel there are examples of mitotic (A) and apoptotic (B) nuclei. The mitotic nucleus is in metaphase; all the chromosomes are aligned but have not yet begun to pull apart. The nuclear envelope of the apoptotic cell has disintegrated, allowing the stained nucleic acid to disperse. Scale bar = 20 μm.

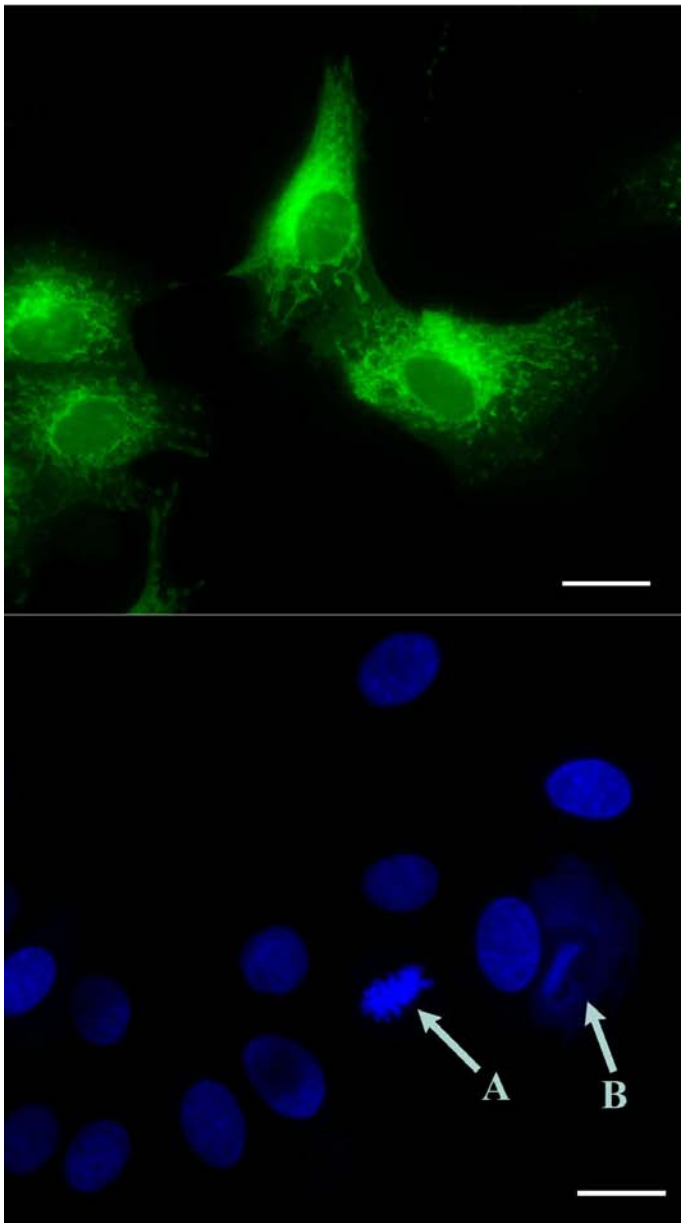
A
B

scanning electron microscope, the resolution limit is approximately 1-5 nm, meaning that specimen details can be resolved at much higher magnifications. Current is passed through coiled copper wire lenses, which focus and magnify the electron beam. The column and specimen chamber are kept under a vacuum to minimize gas molecules that interfere with the mean free path of the electrons. The electrons themselves are generated by a heated tungsten filament, which is part of the apparatus known as the electron gun. Several parameters, such as spot size, current, working distance, and accelerating voltage, determine resolution, brightness, depth of field, and penetration depth of the electrons into the sample. There are trade-offs in each. A lower accelerating voltage, for instance, will not show as much depth but will show fine surface details that are lost when faster-moving electrons do not have the same amount of time to interact with objects on the surface. **Figure 10** shows an SEM of intact HeLa cells, and **Figure 11** shows an SEM of detergent-extracted HeLa cells, where the plasma membrane was removed to reveal internal cytoskeletal structures.

Transmission electron microscopy (TEM) works under many of the same principles as SEM, but instead of scattering off the surface of specimens, electrons pass through thin specimen sections and hit detectors on the other side. TEMs generally operate under a higher vacuum than SEMs, use a higher accelerating voltage, and have a better resolving power at higher magnifications. TEM is used to view internal cellular structures of sectioned material. An example of this type of imaging is shown in **Figure 12**.

Figure 10. Example of scanning electron microscopy (SEM).

These HeLa cells were treated with two types of calcium ionophore (A23187 and ionomycin), drugs which make cell membranes permeable to calcium and other ions. They were imaged under SEM to determine if the drugs had any effect on filopodia formation. The results of this experiment were inconclusive, but micrographs like this one demonstrate the visual effectiveness of cell surface images using SEM. The cells appear three-dimensional, well-contrasted, and in focus. Scale bar = 20 μm.

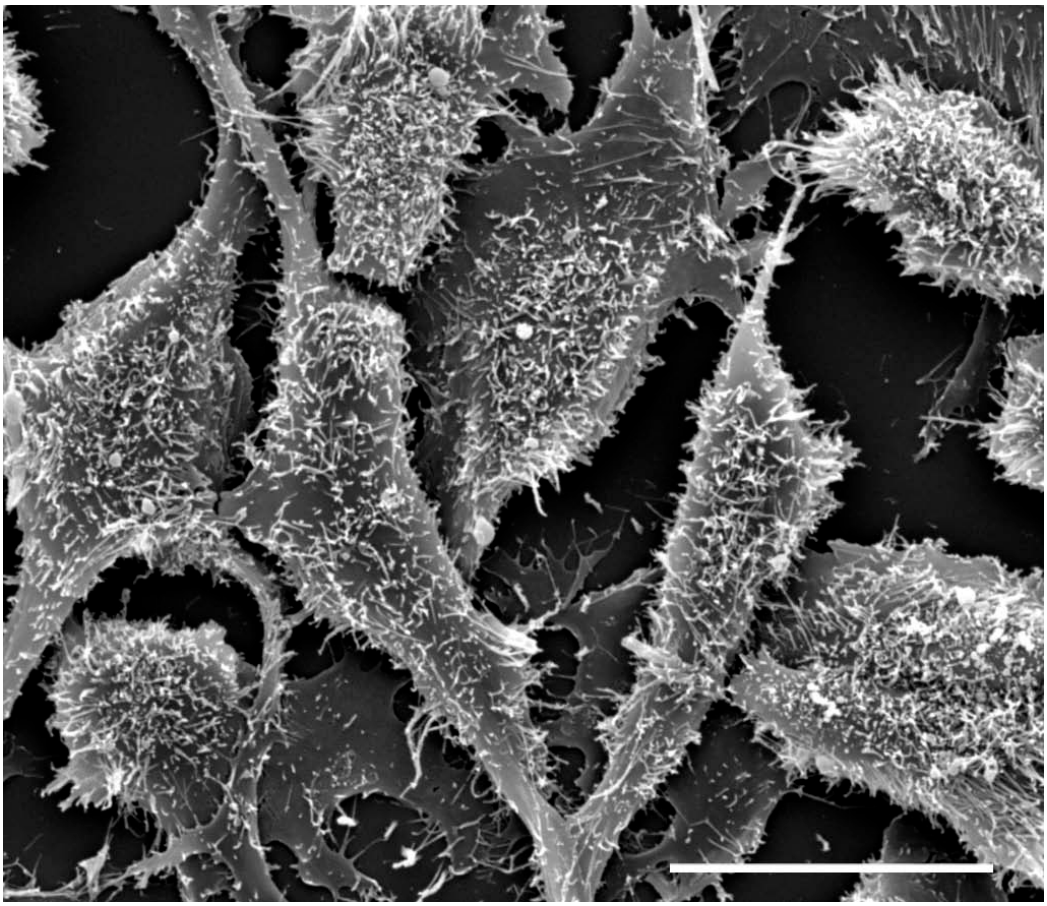

Figure 11. SEM of HeLa cells with plasma membrane partially removed through detergent extraction.

These HeLa cells were treated with Triton X-100, a detergent commonly used to extract cell membranes, immediately prior to fixation. This particular sample was exposed to the detergent for only one minute, which may explain why much of the membrane remained relatively intact – particularly around the main cell body. The lamellipodia, however, are nicely extracted, and show a network of cytoskeletal fibers. Some of these fibers are aligned in the direction of protrusion, while others appear to branch and spread laterally. Scale bar = 20 µm.

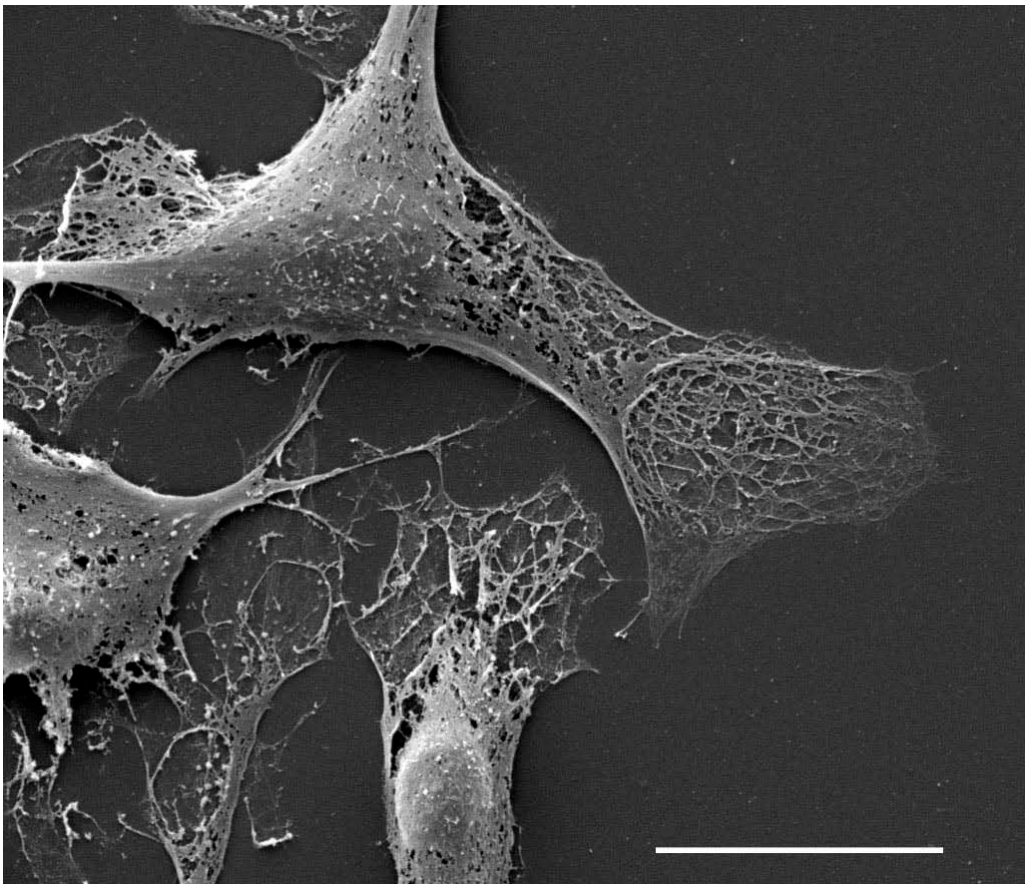

Figure 12. TEM of the margin of an MDCK cell.

Filopodia fragments (A) are visible outside the main region of the cell. Mitochondria (B), the organelles responsible for cellular respiration, are commonly imaged under TEM. Rough endoplasmic reticulum (C) stands out in sharp contrast due to the coating of ribosomes, which appear as tiny, black dots. The cytoplasm contains a high concentration of ribosomes. The Golgi apparatus (D), seen here in cross-section, is structurally comprised of flat, membranous stacks. Vesicles merge and pinch off from this organelle, which sorts trafficked materials. Cytoskeletal filaments (E) are also observed in this thin section, which was taken approximately 550 nm (8 sections deep) from the interface between the cell and the coverslip. Scale bar = 1 μm.

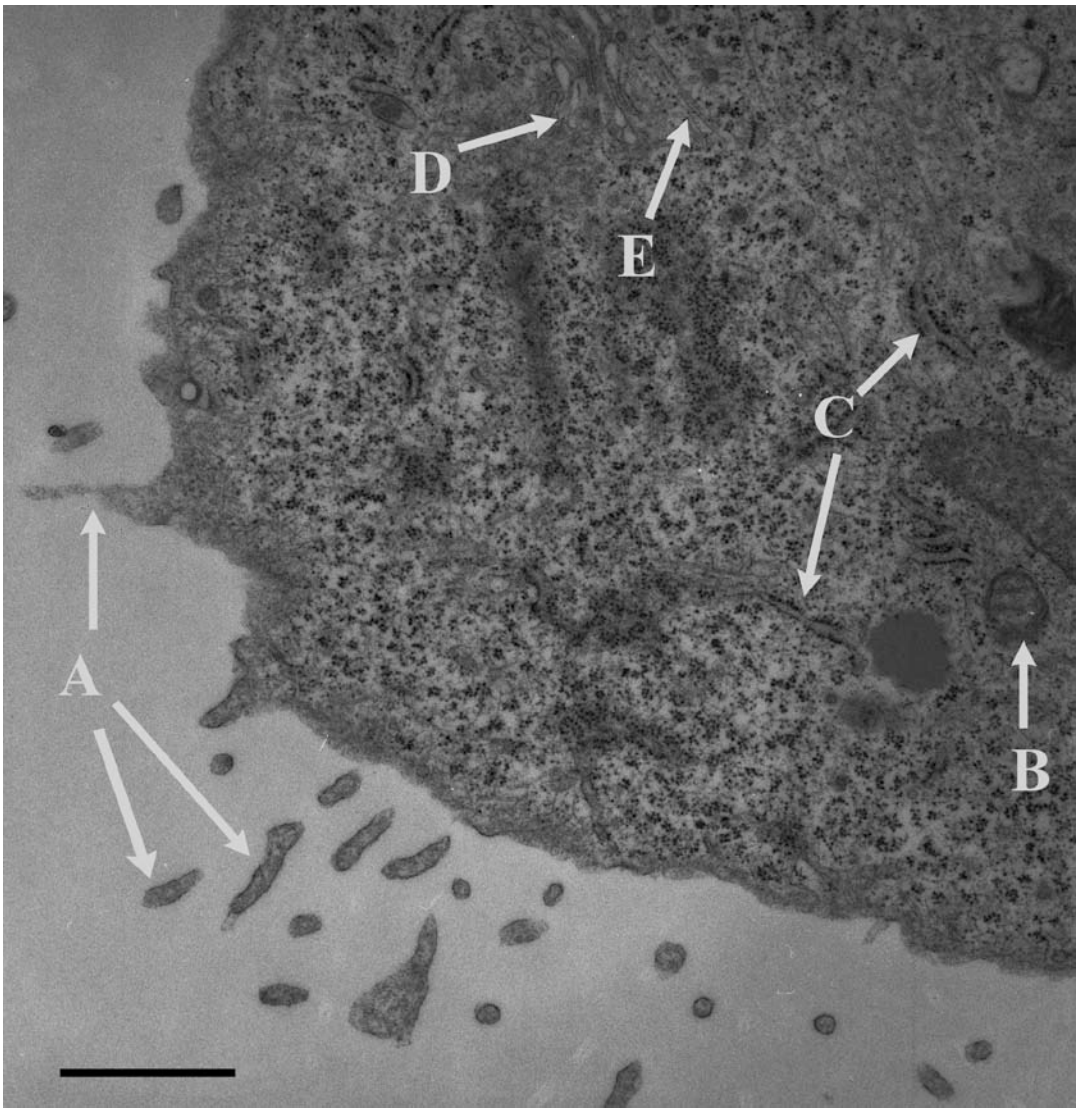
D
E
C
A
B

Cell types used in this study

There are five cell types included in this project that represent very different vertebrates, different locations within the organisms, and three extremely dissimilar functions.

Movement of *Fundulus* keratocytes, epidermal cells from the scales of killifish, is well-documented in time-lapse video microscopy. They are considered one the most rapidly-migrating cells, with crawling velocities of up to 15-25 μm/min. (Burton 1999). Keratocytes are notable for maintaining a consistent velocity and a characteristic, fan-like shape **(Fig. 13)** as they migrate (Wilson et al. 2010). They are responsible for the production of keratin, a relatively hard structural protein. Scales are plucked from live fish immediately prior to the manual dissection of keratocyte-rich tissue, which is not sterile and is therefore used and discarded the same day.

The second cell type is from a line of cells that has been in culture since it was isolated from a woman's vicious cervical tumor in the early 1950's. Henrietta Lacks (the basis of the culture name HeLa) died of the cancer, but she is immortalized in her cell line. These cells are remarkable in their rapid proliferation in culture and apparent inability to senesce. As experimental models for diseases such as polio, they have become a staple of medical and cytological research (Skloot 2010, 4). They are often models for the effects of cytotoxins. HeLa cells **(Fig. 14)** are easy to culture, so much so that mitotic divisions tend to rapidly accelerate mere weeks after the culture is begun. They are also a common

contaminant of other cultures kept in close proximity and manipulated in the same hood space. HeLa cells, like the other migratory cell types, form motility structures such as filopodia and lamellipodia; because they adhere so well to both glass and round therminox coverslips, they are easily cultured and fixed for both SEM and light microscopy. They exhibit slow migration, with leading cells (at the margin of wound areas) achieving velocities of approximately 7 μm/hour (Tountas 2004, Ronot 2000). HeLa cells can migrate individually, but because they populate an area so quickly and usually have neighbors on all sides, they more frequently migrate in groups.

Mesenchymal stem cells isolated from mouse compact bone and bone marrow **(Fig. 15)** are used as another type of motile cell in the process of investigating actin structures like filopodia and lamellipodia. These cells are smaller than HeLa and keratocytes, and require extremely sterile culture conditions. Unlike HeLa cells, which immediately flatten and divide to form a monolayer, these stem cells undergo mitosis at a more modest pace. They sometimes respond poorly to fixation for SEM. The importance of adult stem cells in medical research, already acknowledged to be enormous, is constantly growing. Mouse bone stem cells are used in this study because of their migratory properties, providing another example of crawling cells. However, their motility in vitro is not well characterized in scientific research, which tends to focus more on differentiation and in vivo niche homing. Mouse bone marrow stem cells seem particularly prone to associate in vitro with fibroblasts.

Figure 13. Phase/contrast image showing an example of migratory keratocytes. Scale bar = 10 µm.

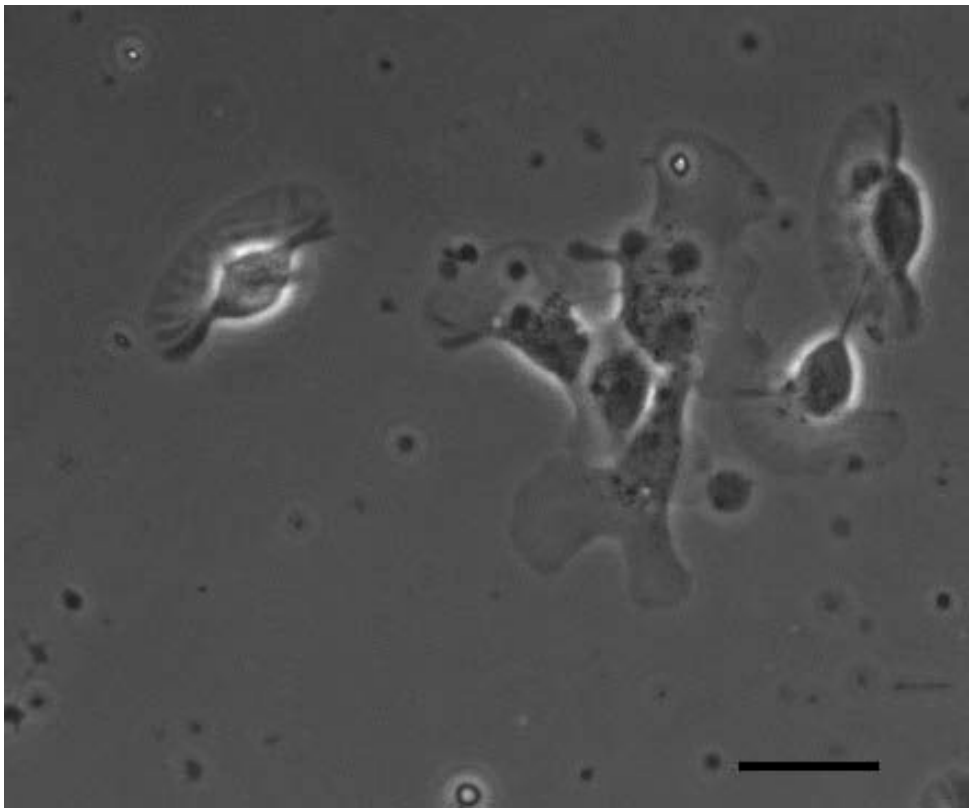

Figure 14. Phase-contrast image of motile HeLa cells.

This image shows two filopodia (A), spreading at the tips to form lamellipodia. (C) shows two nuclei which seem to share common cytoplasm in the same, binucleate cell. Polynucleated HeLa cells are not rare. A retraction fiber (B) extends from the lagging edge of a crawling cell. Scale bar = 20 µm.

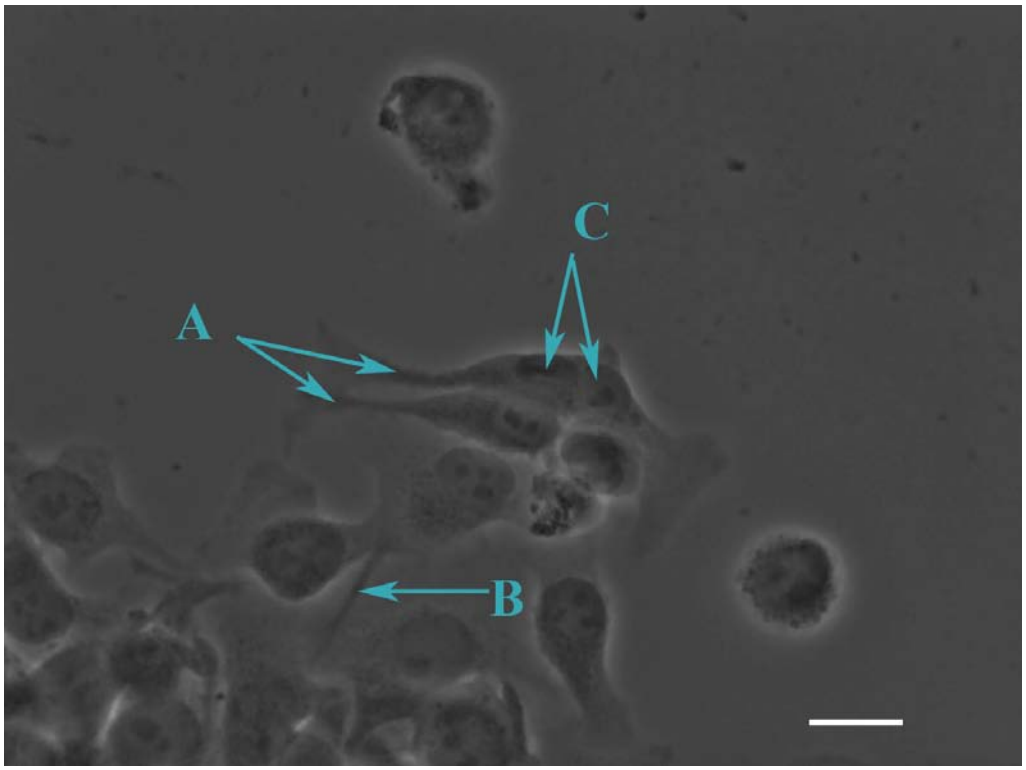
C
A
B

Fibroblasts are mesenchymal cells that produce collagen, an important and abundant structural protein of the ECM. Other molecules of the ECM, such as elastin and the dimeric protein fibronectin, are also synthesized by fibroblasts. Fibroblasts are downstream in differentiation with respect to mesenchymal stem cells, meaning that MSCs have the potential to give rise to them. Fibroblasts form large lamellipodia that can have over ten times the area of the main cell body **(Fig. 16)**. They are important in wound response in vivo, quickly migrating to areas of injury to assist in scar tissue formation. In relation to other migratory cell types, fibroblasts move at an intermediate velocity: approximately 40 μm/hour (Bray 23).

Madin-Darby canine kidney (MDCK) epithelial cells **(Fig. 17)** are a cell line originally isolated in 1958 from the kidney of a cocker spaniel. Like HeLa cells, they form a tight monolayer in culture, and have long been a popular experimental model.

Figure 15. A colony of mouse compact bone-derived mesenchymal stem cells under phase/contrast.

Mouse compact bone MSCs (seen here) and bone marrow MSCs form monoclonal colonies in vitro. Their morphology is considered fibroblastic, making it difficult to determine stem cells from actual fibroblasts, which are also found in stem cell cultures (particularly in the bone marrow). Photograph taken by Anastasia Hyrina at Mount Holyoke College. Scale bar = 50 µm.

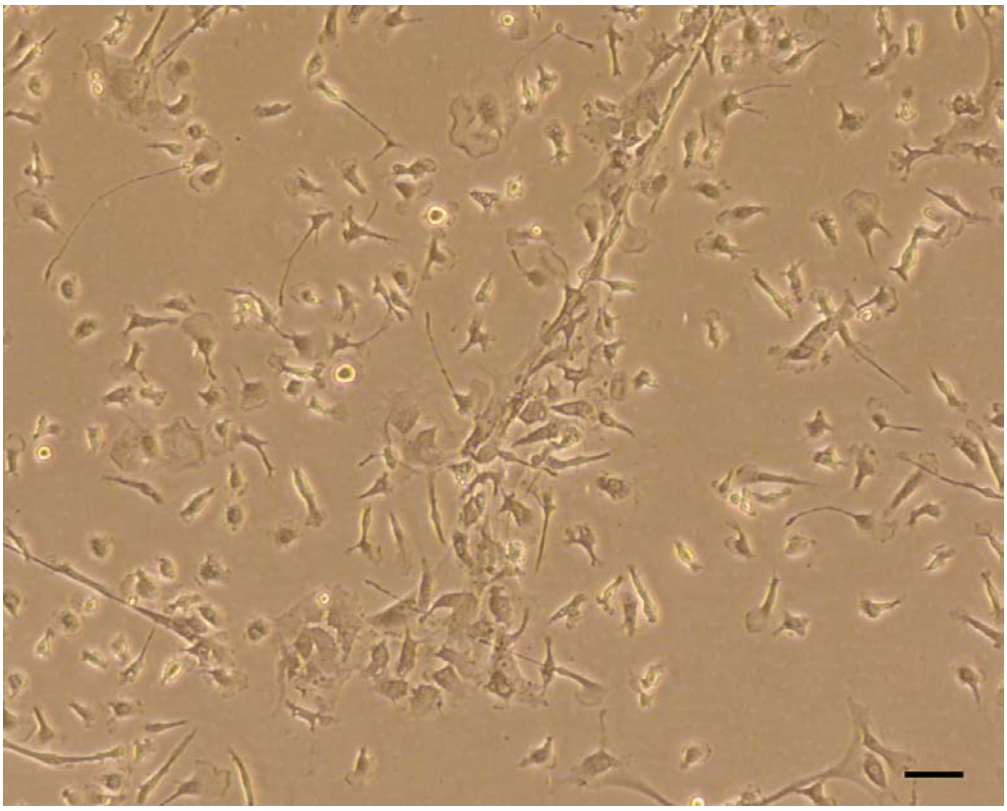

Figure 16. SEM of a migratory fibroblast (a) with labeled structures (b).

This fibroblast, isolated from chronically inflamed (NPC1) mouse bone marrow, was in the process of migrating just before it was fixed for SEM. The lamellipodium (A), complete with plasma membrane ruffling at the leading edge, encompasses a total area approximately 12.5 times that of the main cell body (B). Several retraction fibers are visible in this micrograph, though the thick one (C) in the central-rear of the cell is the most prominent. Scale bar = 20 µm.

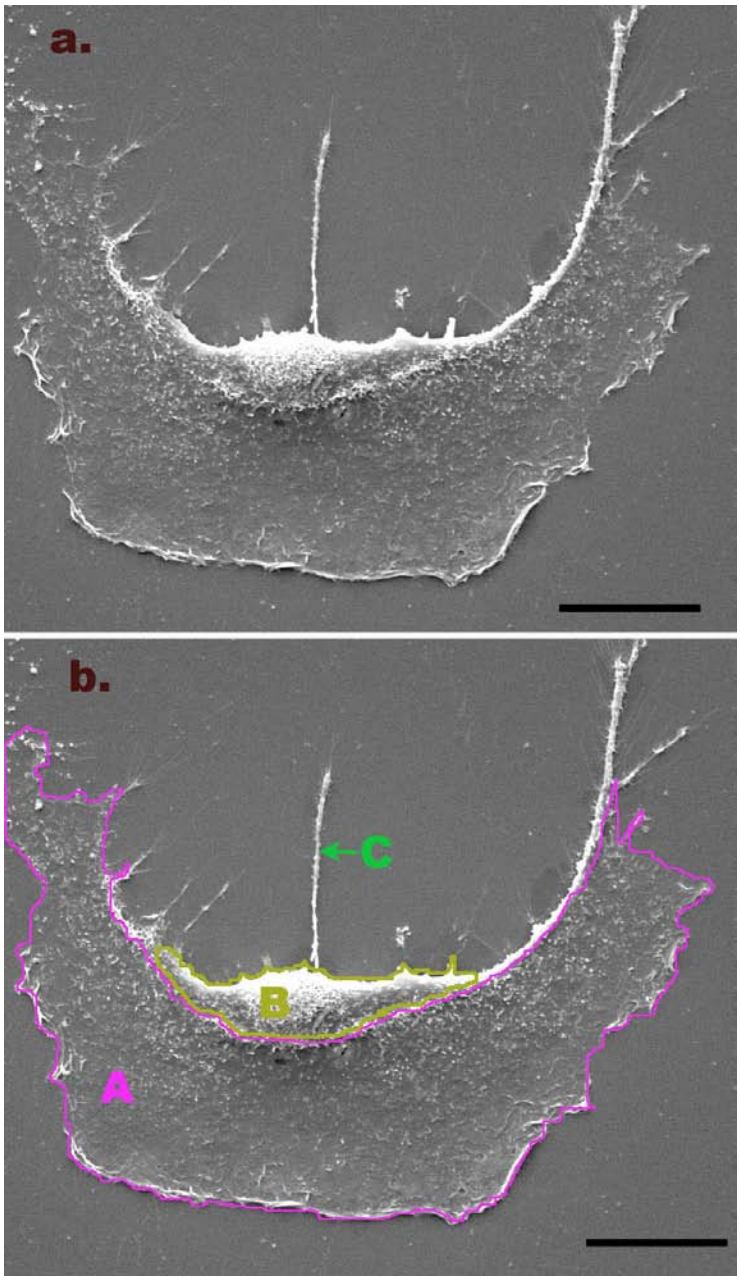
a.
b.
C
B
A

Figure 17. MDCK cells in a monolayer.

MDCK cells form a tight monolayer with neighboring cells. Shown here is one area of the monolayer margin, from which several cells are beginning to extend. The round cell near the center of the image is covered in hemispheric blebs, indicating that it is likely mitotic. Scale bar = 20 µm.

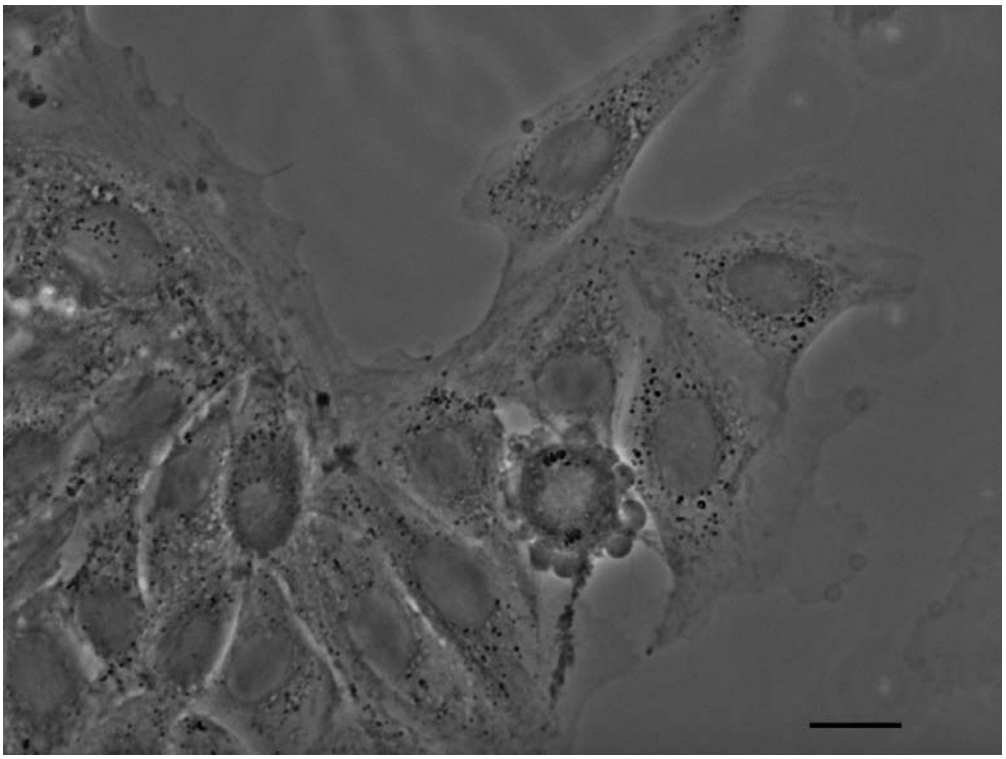

There is a wealth of information about cell migration. It is understood that migrating cells form filopodia and lamellipodia; that they gain traction by adhering to their substrate; and that membrane ruffles occur when reorganization of actin filaments disrupts the smooth appearance of the membrane covering them. However, it is useful to actually see these phenomena in a collection of micrographs representing a diverse array of migratory cell types. Imaging these five cell types in a variety of different ways is the basis of this investigation. Information about the way cells crawl, from cytoskeletal organization to overall morphology, is gained by taking and analyzing hundreds of micrographs that each contribute something new to the story.

METHODS AND MATERIALS

Each cell type had its own medium, substrate, and sterilization requirements in order to maintain vitality, prevent differentiation, and/or plate cells for imaging. The following section details culturing procedures and media recipes.

Fundulus keratocyte culture methods

Scales were gently taken from live adult killifish (*Fundulus heteroclitus*) using forceps, in a way that did not harm the animals. Upon removal from the fish, the scales were placed immediately into a glass dish containing room-temperature culture medium (90% Liebovitz's L-15 and 10% Gibco fetal bovine serum (FBS)). Under the dissecting microscope at approximately 6x, keratocyte-rich tissue was isolated from the base of the hard, keratinized scale using two forceps, one in each hand. It took approximately three scales' worth of tissue per trial (i.e. per coverslip) to achieve sufficient culturing concentration. The scales were discarded once they were stripped of living tissue. Glass pipets were used to suction the tissue out of the glass dish, minimizing as much as possible the volume of medium taken along with the solid particles. The tissue and small amount of medium was pipetted into and out of a plastic, non-sterile microfuge tube several times to mechanically loosen the clumps of tissue. The microfuge tube was then shaken vigorously for ten seconds with the same goal.

One trial involved vortexing the tissue in a trypsin/EDTA digestive solution for fifteen seconds before pipetting the samples back into medium. The whole process was non-sterile, so the samples had to be used the same day they were taken from the fish.

After allowing approximately one minute for the tissue to settle at the bottom of the tube, the tissue was suctioned up and placed across 3 to 5 square glass coverslips which had already been placed into plastic petri dishes lined with strips of parafilm to facilitate eventual transportation out of the petri dish. Adhesive properties of any small amount of liquid medium spilled onto the bottom of the petri dish would otherwise make the coverslips stick there, and make removing them difficult. Additionally, three small shards of broken coverglass had been pre-placed on each coverslip so that the placement of a top coverslip would not crush the cells. Once the tissue was on the coverslips, a small amount of clean medium was added. The top coverslip was then placed carefully on the glass shards, forcing the tissue-containing medium to spread evenly across the whole coverslip. Finally, a wet piece of filter paper was placed on the cover of the petri dish to create a moist chamber environment for these coverslip sandwiches. The coverslips were left untouched at room temperature for a minimum of three hours.

For SEM preparation, round Thermanox coverslips were used instead of glass coverslips. They were cleaned with 95% ethanol, rinsed and dried thoroughly, and placed in a moist chamber petri dish on strips of parafilm. Two

drops of 0.1% poly-L-lysine solution in 0.1M sodium phosphate buffer were pipetted onto each coverslip. The coverslips were left at room temperature for one hour, rinsed with distilled water, dried by touching the edge to a laboratory wipe, and stored in the refrigerator in a covered, plastic 12-well plate. The keratocyte-rich tissue was isolated, mechanically separated, and placed on the coverslips with medium as described above. They were left in the moist chamber 12-well plate at room temperature for a minimum of five hours, as the fixation procedure for SEM requires that the cells be highly adherent to the coverslip.

HeLa culture

Cryogenically frozen HeLa cells were thawed and pipetted into RPMI complete medium at a ratio of 1 mL cell suspension: 4 mL medium. RPMI complete medium contained 88% RPMI, 10% FBS, and 1% each of penicillin-streptomycin antibiotic solution and L-glutamine. The 5mL of cell suspension was pipetted into a T-25 culture flask and incubated at 37 degrees Celsius with a loose cap. The cells began to form a monolayer within one day, and had to be split and given fresh medium at least once every three days. For plating, cells were transferred into a T-75 culture flask at the ratio of 3 mL cell suspension: 12 mL fresh medium. 1 mL of the remaining cell suspension was pipetted back into a clean T-25 with 4 mL medium to keep the cell line growing after plating. After approximately four days, the cells in the T-75 flask were trypsinized, re-suspended, and pipetted onto sterile Thermanox coverslips in a 12-well plate. After one day the monolayer re-formed on all the coverslips and the

cells were ready to be fixed. Sterile procedures were followed at all times with this cell line.

Mouse mesenchymal compact bone and bone marrow stem cells

Dr. Lamis Jarvinen and her lab team isolated and cultured the stem cells used in this study.

The femurs and tibias of humanely sacrificed mice were harvested and trimmed. Marrow was flushed out by injecting the femoral and tibial shafts with IMDM culture medium + 2% FBS. Using the syringe, culture medium and marrow cells were drawn up and down several times to mechanically separate the tissue into a single-cell suspension. Aliquots of this suspension were diluted 1:50 in 3% acetic acid with methylene blue. Cell counts of nucleated cells were obtained using a hemocytometer. The expected yield was 3.0-5.0 x 10^7 cells per mouse (two femurs and two tibias).

Compact bone samples were also obtained from clean, freshly-harvested femurs and tibias. They were placed inside a mortar with a buffer solution of PBS, 2% FBS, and 1mM EDTA. Bones were cracked open using a pestle, and released bone marrow was pipetted off. Compact bone fragments were transferred to a dish containing 0.25% Collagenase Type 1, PBS, and 20% FBS for five minutes. They were ground into smaller pieces with a scalpel. Once transferred into a fresh Collagenase solution, they were placed into a shaking 37°C water bath, set at maximum speed, for 45 minutes.

The same PBS + EDTA buffer was added to the container and the mixture

was poured twice through a 70μm cell strainer. The wash was then centrifuged at 1200 rpm for ten minutes at room temperature. The pellet was resuspended in Complete MesenCult Medium® (mouse), diluted in acetic acid as before, and cell count was determined. The expected yield was 1.5-3.5 x 10^6 cells per mouse. Cells were expanded in T-25 flasks containing Complete MesenCult Medium® before plating in a 6-well dish at 5.0 x 10^5 cells per well. Cells were cultured for ten days at 37°C in 5% CO_2. They were then stained with Giemsa staining solution in order to count the number of colonies present, and to assess the sizes of the various colonies under the inverted compound culture microscope. For SEM, the cells in a T-25 flask were rinsed with sterile PBS, trypsinized, resuspended, and plated in a 24-well plate on small Thermanox coverslips at a concentration of approximately 1 x 10^5 cells per well.

MDCK culture

MDCK culture procedures matched those for HeLa culture, and were carried out by Sue Lancelle of the Biology Department at Mount Holyoke College.

Plasma membrane extraction

Keratocytes allowed to grow on small, poly-L-lysine coated Thermanox coverslips for six hours were rinsed once briefly with PBS and then exposed to a detergent solution (0.01% Triton x-100, 2.5% glutaraldehyde, and 0.01M phalloidin in PBS) for 1.5 minutes. The phalloidin was added to the solution in order to help maintain the integrity of the actin network during the extraction

procedure. After the detergent solution was removed using a disposable plastic pipet, the coverslips were rinsed 3 times with PBS and immediately placed into primary fixative solution (described below).

Cultured HeLa cells were extracted using the same detergent solution as described above, minus phalloidin. Three non-coated Thermanox coverslips were used; one was exposed to the detergent for one minute, the second for three minutes, and the last for five minutes. Like the keratocytes, they were rinsed 3 times with PBS and immediately fixed for SEM.

Fluorescent staining

Coverslips containing keratocytes were examined under the culture microscope to detect adherent cells and to evaluate their readiness for fixation. The presence of healthy-looking tissue sites surrounded by cells displaying filopodia and/or lamellipodia indicated that the cells had been allowed enough time in culture. The coverslips were rinsed twice briefly with room-temperature PBS buffer (pH 7.2) by dipping them in coplin jars before they were transferred to a coplin jar containing room-temperature 4% formaldehyde in 1x PBS for ten minutes.

After the primary fixation, the coverslips were rinsed twice in PBS for one minute each. They were then transferred to a coplin jar containing acetone stored in the freezer at -20 degrees Celsius. The coplin jars containing the cells went back into the freezer for three and a half minutes to extract the plasma membrane. After they were air-dried by holding them with forceps so that air could circulate

across both sides, the coverslips were placed cell-side-up in a moist chamber (petri dish with damp filter paper) and stained by placing three 50-microliter drops of 1.0 micromolar Alexa Fluor 546-phalloidin (rhodamine phalloidin) solution onto them so that each portion of the coverslip area was bathed in stain solution. They were left to absorb the stain for 20 minutes at room temperature, inside a closed box so that no light would reach them.

After the 20 minutes, the coverslips were rinsed twice briefly with PBS and dried by touching a laboratory wipe to the edges. The non-cell side was wiped down. A small drop of anti-fading solution (to retard the photobleaching of the fluorochrome) was placed on each glass slide using a disposable plastic pipet. The slides were kept in the dark when not being imaged under the microscope.

The protocol for fluorescent staining of HeLa cells was nearly the same as the protocol for keratocyte staining, except that the coverslips remained in acetone for five minutes instead of 3.5.

SEM fixation

Cells intended for SEM were left in culture longer (five to seven hours) in order to ensure maximal adherence to the poly-L-lysine coverslips. Whether the cells were extracted or not, the protocol remained as follows:

Medium was removed using a disposable plastic pipet, and the coverslips were rinsed twice briefly with PBS. 1 mL of a primary fixative solution was then added (2.5% glutaraldehyde in 1M Na Cacodylate buffer, pH 7.2). The cells were left to fix for 45 minutes in the refrigerator with parafilm around the edges of the

12-well plate. Afterward, they were rinsed 3 x 5 minutes with 1M Na Cacodylate and put into a post-fixative (or secondary fixative) solution comprised of 1% Osmium Tetroxide in 1M Na Cacodylate buffer. After 20 minutes, they were rinsed 3 x 5 minutes with distilled water. They then underwent a series of ethanol changes, beginning with 50% ethanol and then going to 70%, 80%, 90%, 95%, and finally 100%. The cells soaked in each solution for 5 minutes. At the 100% step, there were three changes at 5 minutes each.

The 12-well plate was wrapped in parafilm and placed in the refrigerator at 4 degrees Celsius until the cells could be critical point dried. After critical point drying, the coverslips were sputter-coated with gold for 90 seconds.

The SEM fixation of HeLa cells matched that of keratocytes, except that there were three initial rinses with PBS. Another difference is that these rinses - as well as the preceding media removal - were carried out in a laminar flow hood to maintain the sterility of the HeLa culture. They were then brought to the electron microscopy preparation room for immediate placement into primary fixative.

The protocol for stem cell fixation for SEM was the same as that used for keratocytes.

Fixation of MDCK cells for TEM

Cultured MDCK cells were seeded at 200,000 cells per mL (coverslips 1-3) and 270,000 cells per mL (coverslips 4-6) on large Thermanox coverslips, each with an asymmetrical notch to indicate cell side up vs. cell side down **(Fig. 18)**. All six wells of the plate were used. Cells were rinsed briefly once with PBS,

then fixed with 2% glutaraldehyde in 0.1M Na Cacodylate buffer (pH 7.2) for one hour. They were rinsed 3 x 5 minutes each with 0.1M Na Cacodylate buffer. They were post-fixed in 1% Osmium Tetroxide in 0.1M Na Cacodylate for one hour. After being rinsed with distilled water 3 x 5 minutes, the cells were stained *en bloc* for 30 minutes with 1% uranyl acetate. They were dehydrated five minutes each in an ethanol series: 30%, 50%, 70%, 90%, and 3 x 100%. The cells were infiltrated with Spurr's Resin using the following formula: 30 minutes of 2:1 ethanol:resin; 1:1 ethanol:resin (another 30 minutes); 1:2 ethanol:resin (30 minutes); and finally two changes of 100% resin (for one hour, and then overnight). The resin-containing plate was gently shaken occasionally. After infiltrating overnight, the coverslips were transferred to aluminum weighing pans – cell side up – and covered with a thin layer of resin. Care was taken to push the coverslips down along the edges, so as not to remove fixed cells, in order to minimize resin beneath the non-cell side. The six pans were put into a vacuum oven at 50 degrees Celsius for 15 minutes, then polymerized at 70 degrees Celsius overnight.

After peeling the aluminum away, the hard resin wafers were gently heated by placing them on a paper towel that rested on a hot plate (setting 2). When the resin began to soften, extra resin was cut away using a razor blade. This took many cycles of cutting and re-heating, as the resin cooled and re-hardened within a matter of seconds. Once the edge of the coverslip was exposed, the razor

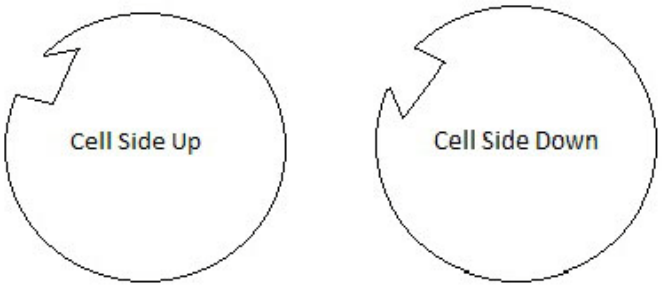

Figure 18. Positioning of trapezoidal notch in large Thermanox coverslips for TEM to indicate cell side vs. non-cell side.

blade was worked in between the cell side of the coverslip until there was enough to grab by hand. While the wafer rested on the hot plate to keep it pliable, the coverslip was gently separated and pulled off. Both the remaining resin wafer (with cells embedded) and the separated coverslip were examined using the inverted culture microscope to determine the quality of the cells and whether there were any left behind. Many cells were observed in the resin, and a high percentage of them were flat. Stained organelles were visible, indicating good fixation and preparation. Very few intact cells were observed on the coverslips; what remained appeared to be mostly cellular debris.

Pieces of resin, approximately 4mm in diameter, found to contain a high concentration of cells were cut away from the wafer using a jewelers' saw and mounted on plexiglass rods using epoxy glue, cell-side-up. After the epoxy dried

for more than 12 hours, the specimens were trimmed in an asymmetrical trapezoid measuring no more than 1mm on the longest side. They were thin-sectioned using an ultramicrotome, with the very first sections (the most likely to contain lamellipodia) captured and placed on grids.

Some sections were placed on glass slides and stained with Toluidine Blue stain, and imaged at 100x and at 400x under phase/contrast **(Fig. 19)**. The cells were evaluated for concentration and appearance: whether or not they appeared to have a normal morphology, whether organelles were present, etc.

The grids selected for TEM were post-stained, section-side-up, using 2% aqueous uranyl acetate (40 minutes) and Reynold's lead citrate (7 minutes). They were rinsed in distilled water between the uranyl acetate and the lead citrate, and immediately after the lead citrate to avoid precipitate formation.

Imaging

Keratocyte slides were imaged using the Olympus BH-2 compound microscope. Four time lapse movies were created by setting the PixeLink digital camera to take still frames at regular intervals, over various total time lengths. The frame intervals used were 20 seconds, 10 seconds, 5 seconds, and 2 seconds. These stacks of images were turned into movies using ImageJ software.

HeLa cells and MDCK cells were imaged during fluorescent procedures using the Olympus BH-2 compound/fluorescence microscope. Phase/contrast photographs were taken alongside fluorescent images for comparison purposes and to later create image overlays. Photographs were taken using a PixeLink

digital camera. Rhodamine-phalloidin-stained keratocytes were imaged using the Nikon Eclipse TE2000-U fluorescent microscope with a MetaVue digital camera. All samples fixed for SEM were imaged using the FEI Quanta 200 scanning electron microscope. All samples fixed for TEM were imaged using the Phillips CM 100 transmission electron microscope.

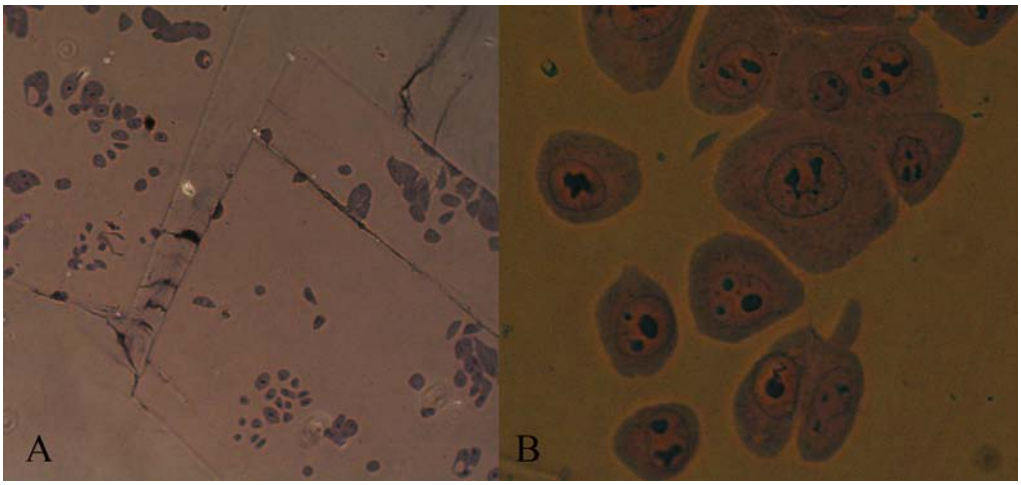

Figure 19. Resin-embedded, thin-sectioned MDCK cells stained for phase/contrast microscopy.

These were test images taken to determine whether or not cells were present in the resin, approximately how many there were, and whether or not the cells appeared normal and intact. The cells in Panel A were viewed under 100x magnification and those in Panel B under 400x. Panel A shows that there are several colonies of cells, and Panel B shows that these cells have intact nuclei and what appears to be a typical cellular morphology. On the basis of these images, the decision was made to continue creating thin sections for the TEM experiment.

Working with images using software

Fluorescent images were modified using Adobe Photoshop® to adjust exposure and restore color. Arrows and labels were added in as needed, and images were cropped and resized to create montages. ImageJ® software was used to compile serial images into time-lapse videos, and also to analyze a fibroblast SEM to determine the areas of the lamellipodium and the main cell body **(Fig. 16)**.

RESULTS

Lamellipodia show both continuity and variability across cell types **(Fig. 20)**. A common feature of lamellipodia - regardless of cell type - is that these structures are always thinner than the main cell body, which rises further off the coverslip. This is evident from viewing SEMs **(Fig. 21)**, which – especially for objects as small as individual cells – have good depth of field.

A defining characteristic of lamellipodia is that they have a large area, but the approximate ratio of lamellipodia: cell body area varies across the different cell types **(Fig. 22)**.

Morphology also has commonalities and differences across cell types. Ruffling is a characteristic of keratocytes and fibroblasts, as well as the slower-moving cells in this study **(Fig. 23)**. Once a keratocyte breaks free of surrounding cells in the tissue mass, it has a single, large lamellipodium that has a characteristic shape **(Fig. 24)**. HeLa cells display no uniformity in overall morphology when crawling in a group or alone **(Fig. 25)**, nor do MDCK cells **(Fig. 26)**.

Filopodia vary in size and internal structure, and are observed in different situations. Filopodia are, by definition, thin and long - though thickness and length vary, not necessarily across cell types but according to growth conditions, apparent function, and level of environmental stress. Micrographs of filopodia

show them to have different lengths, dependent upon the amount of time between initial growth and metabolic arrest due to fixation **(Figs. 27 and 28)**.

Filopodia can be flat and adherent to the substrate, but can also be projected upwards. They can bend and curve **(Fig. 29)**. Sometimes filopodia adhere and then proceed to form lamellipodia to initiate crawling **(Fig. 30)**.

Filopodia show different cytoskeletal organization across cell types. Some are arranged in classic, parallel bundles **(Fig. 31)** while others contain microfilaments that intersect non-uniformally **(Fig. 32)**.

When there is a wound in a monolayer of HeLa cells, filopodia are sent out into the depopulated area **(Fig. 33)** before the cells begin to crawl there. Stem cells seeded at low concentrations appear to have more filopodia, perhaps because they need to extend further outward in order to sense chemical messages from neighboring cells. These suggest a largely sensory role for filopodia in the cell types used in this investigation.

In stem cells from mice with an intracellular cholesterol trafficking disorder, there seem to be more than the usual number of filopodia. These filopodia also tend to be abnormally long **(Fig. 34)**.

Figure 20. Lamellipodia show both continuity and diversity across cell types.

Panels A (rhodamine-phalloidin stain) and B (detergent extraction) show lamellipodia in HeLa cells. These lamellipodia are more elongated than those of the keratocytes (C and D) and the stem cells (E and F). The keratocytes in panel D are still in the process of emerging from the margin of a clump of cells, while the keratocyte in image C has successfully migrated away and has a broader, fuller lamellipodium. The stem cells seen in panels E and F are from mouse compact bone and bone marrow, respectively. Scale bar = 10 μm.

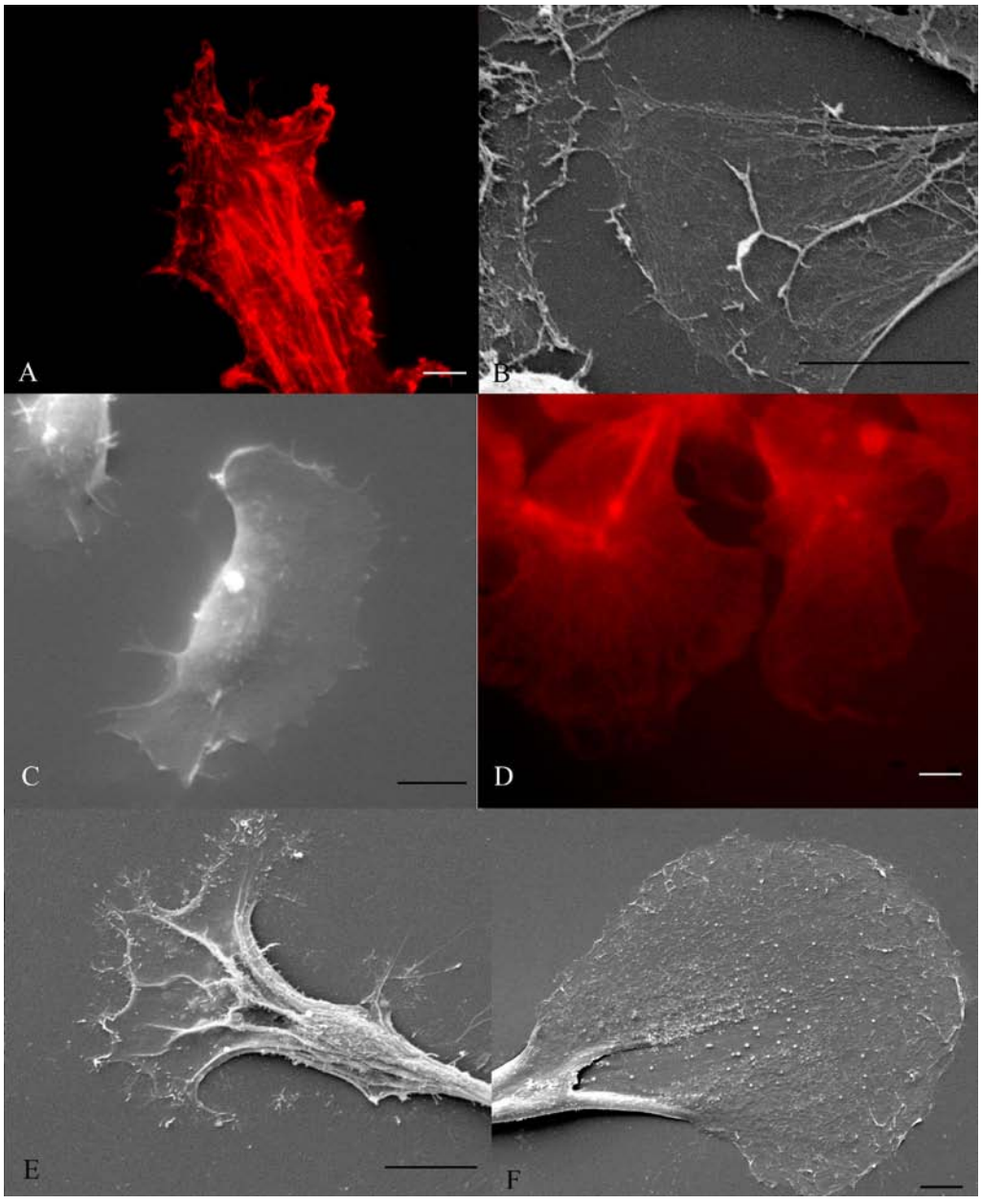
A
B
C
D
E
F

Figure 21. Detergent-extracted HeLa cells with round cell bodies and flat lamellipodia.

The main cell body (A) of the cell with arrows, like those of other cells in this image, is round and rises off the coverslip vertically. Conversely, its lamellipodium (B) is flat, adherent, and horizontally spread. Scanning electron microscopy is a good way to view this phenomenon, since the microscope – particularly at this relatively low magnification – has good depth of field. The closer the region of the cell is to the electron source (i.e. the higher it sits from the coverslip), the brighter it appears. Scale bar = 50 µm.

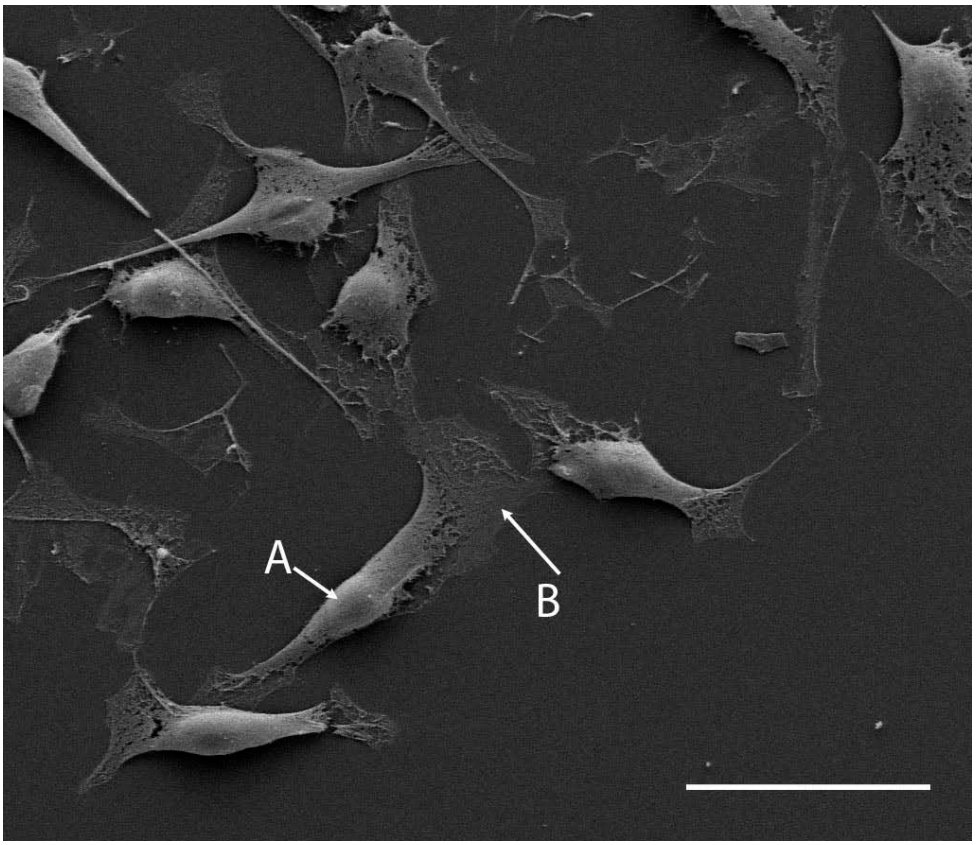
A
B

Figure 22. Different cell types have different ratios between the area of their lamellipodia and the area occupied by the main cell body.

The typical area occupied by lamellipodia (A) changes across cell types, as does the ratio of lamellipodia area: cell body area. The shape of the lamellipodia's span with regards to the main cell body (B) is also variable. The stem cell (4) has a lamellipodium that extends from all sides of the cell body, while the rear-most edges of the keratocyte's lamellipodium (2) are approximately perpendicular to the direction of migration. The sides of the fibroblast lamellipodium (1) extend away from the cell body on what appear to be stress fibers that arc backward on the trailing edge. The HeLa cell (3) has a much larger cell body that is roughly equal in area to the lamellipodium. Retraction fibers (C) remain prevalent in many images of crawling cells. Scale bar = 10 μm.

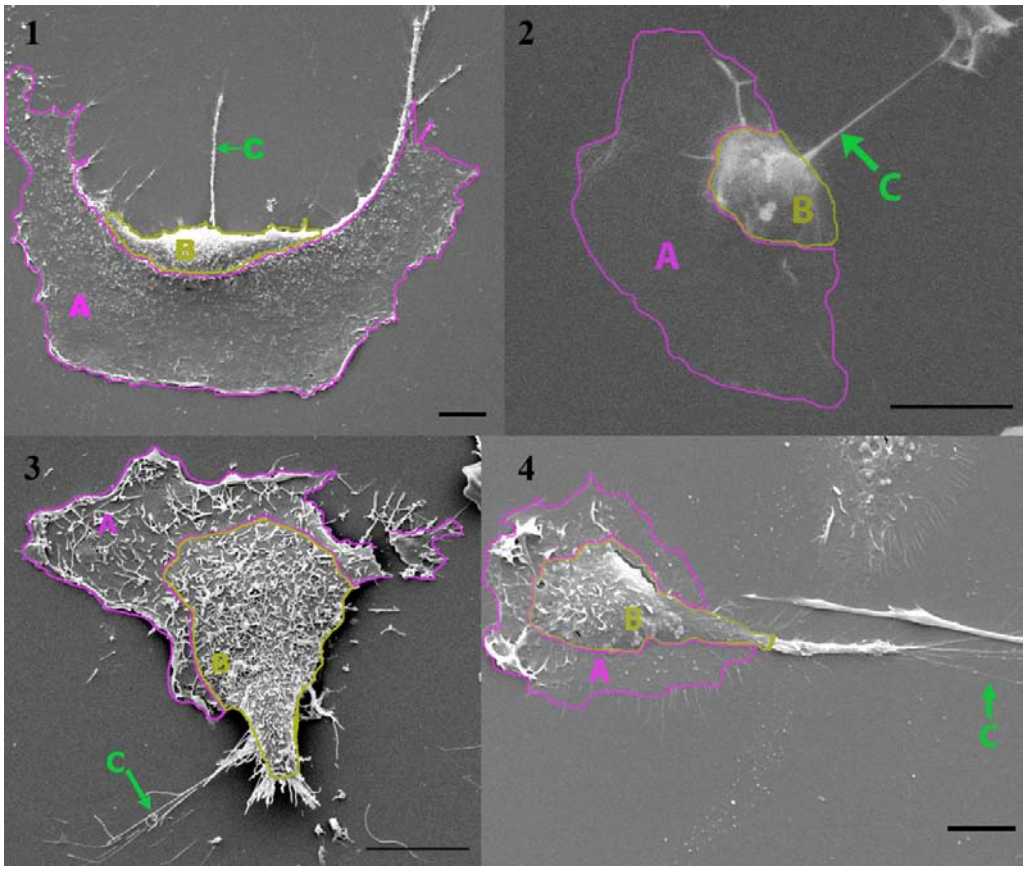
1
C
B
A
2
C
B
A
3
A
B
C
4
B
A
C

Figure 23. Ruffling along the leading edge is a common phenomenon in a variety of migratory cells.

Quicker-moving cells, like fibroblasts (A) and keratocytes (C), are widely known to have ruffling that occurs at the very leading edge. However, slower-moving cells like mesenchymal stem cells (B) and HeLa cells (D), also display this phenomenon. The white arrows show regions along the leading edge where the membrane appears to lift off from the substrate. SEM is a good way to view ruffling, since raised areas appear brighter. Scale bar = 10 μm.

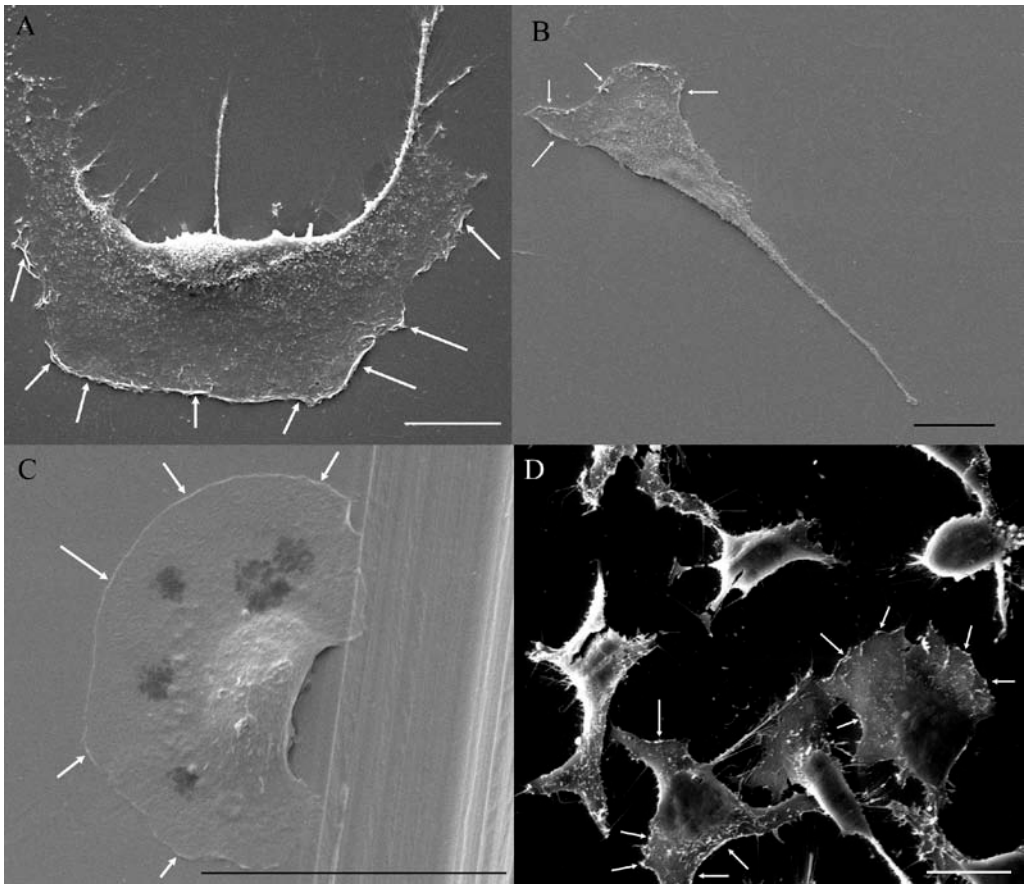
A
B
C
D

Figure 24. Migratory keratocytes have a characteristic morphology.

Keratocytes that have left the cell clump to migrate independently (white arrow) display a characteristic, fan-like shape. The rear-most edges of their lamellipodia are perpendicular to the direction of migration, and evidence of membrane ruffling is visible even in this single, still frame taken under phase/contrast. In this type of view, ruffling is observed as dark, parallel lines on the lamellipodium. This image also contains cells that are almost completely independent (white-and-black arrows) from their neighbors, as well as marginal cells (black arrows) that are still in the process of forming lamellipodia to migrate away. Scale bar = 10 μm.

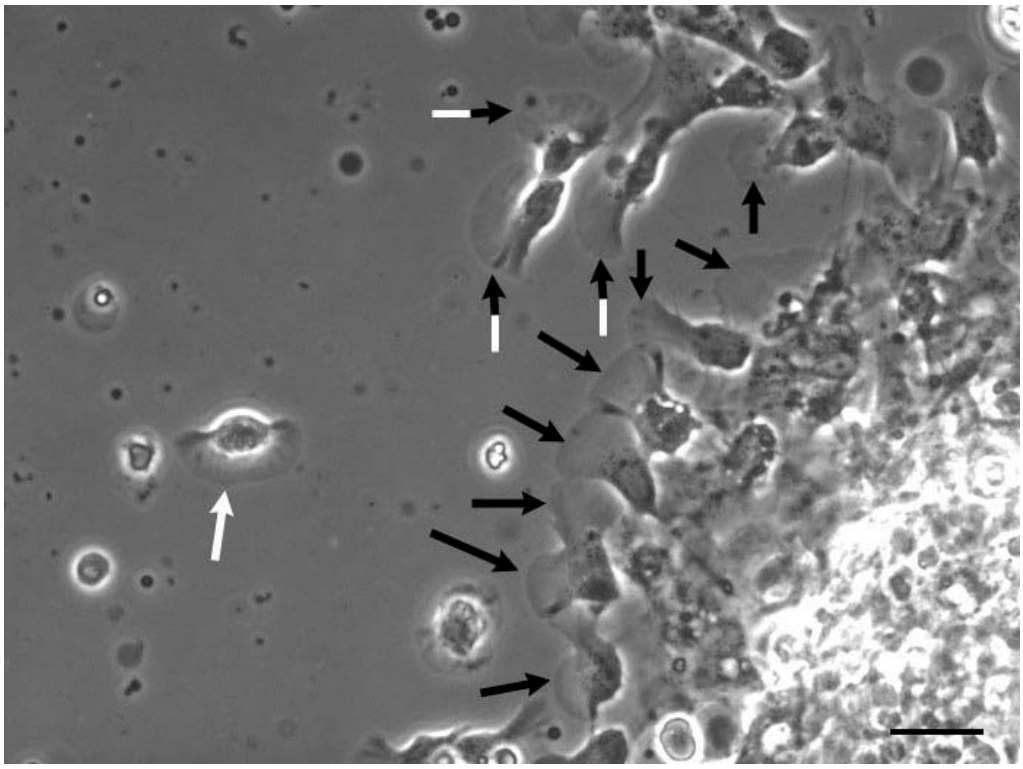

Figure 25. Collectively migrating HeLa cells do not have regular morphologies.

HeLa cells do not form uniquely familiar shapes that render them immediately recognizable. Trained observers can identify them based on other characteristics, but – as seen in this fluorescence/phase overlay image of HeLa cells moving into a gap in the monolayer – overall shape is neither uniform nor defining. One thing to note in this figure is that these cells are migrating collectively as part of the monolayer margin, so it is impossible to compare them against keratocytes, which obtain a familiar shape once they can move freely from their neighbors. Scale bar = 20 μm.

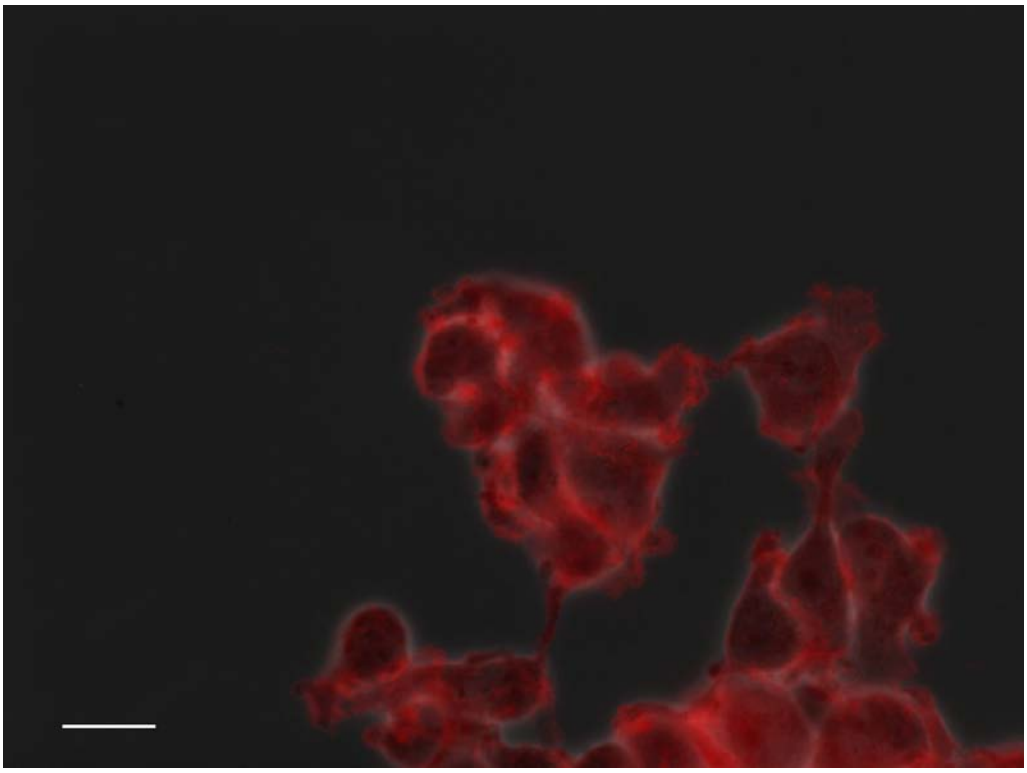

Figure 26. MDCK cells migrating individually have no particular, unique morphology.

The cells in these panels are not attached to the monolayer, but – like HeLa cells - they do not display a common morphology. These are overlay images of phase/contrast micrographs superimposed on fluorescent micrographs. The fluorophore is DiOC6, which stains mitochondria and endoplasmic reticulum. These images were taken as part of a separate study, and are used here to support the point that MDCK cells do not have a common, characteristic shape. Scale bar = 10 μm.

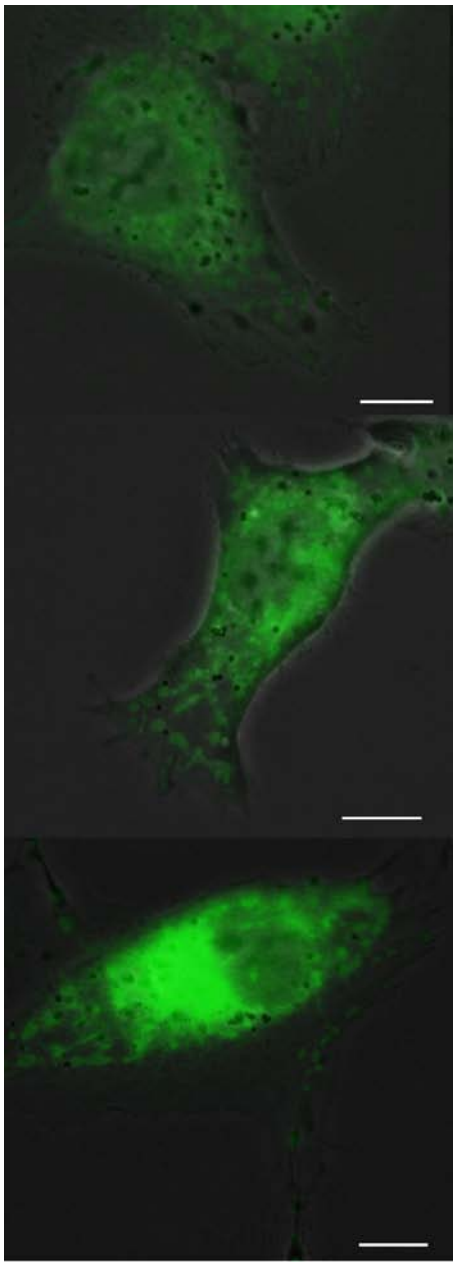

Figure 27. HeLa monolayer containing a cell with a relatively long filopodium.

A round cell (circled) sends out a filopodium whose purpose is probably to find an unoccupied area of the coverslip upon which to settle and adhere. When a HeLa cell is not in contact with the substrate, its behavior and morphology are different from adherent cells in the monolayer. HeLa cells that are blocked by other cells from adhering to the coverslip seem to have a high degree of filopodial growth. This monolayer is so confluent that all the space is taken; the culture was beginning to overgrow before it was fixed. The flatter cell in the upper right corner also has a filopodium, but it is much shorter than the one in the center.

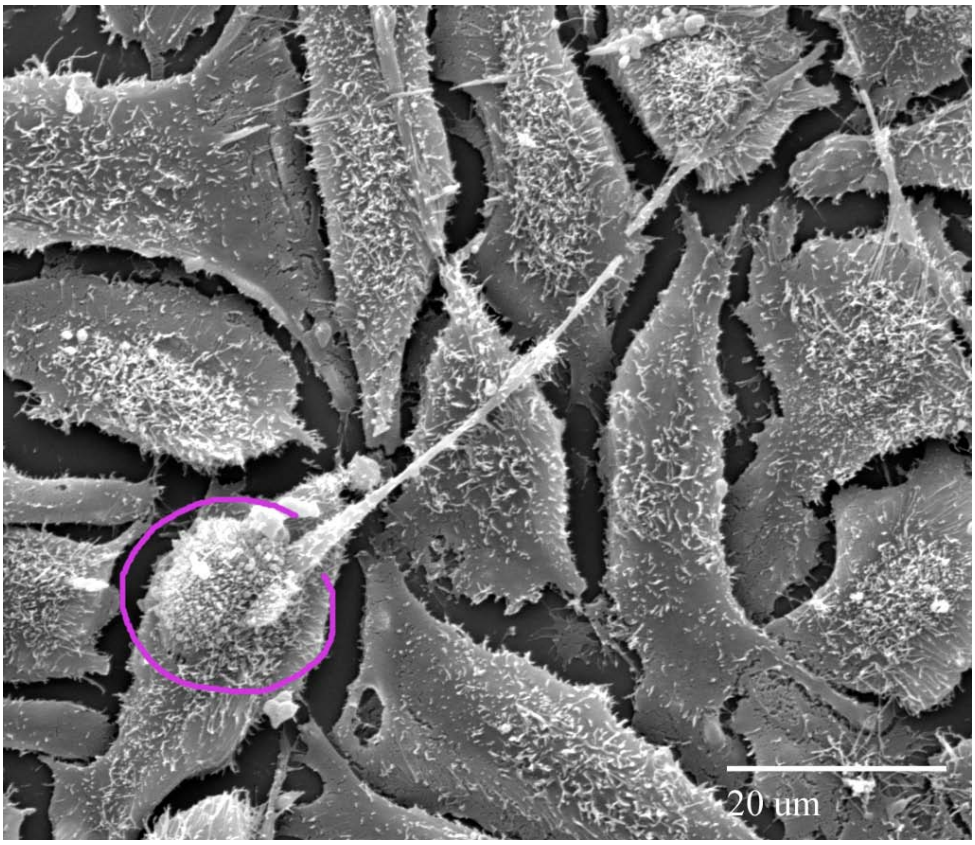
20 um

Figure 28. HeLa cell with a relatively short filopodium.

The adherent cell seen here with a shorter filopodium is beginning to crowd over its neighbor. Again, the purpose of the filopodium seems to be to sense the environment and to find an area of less dense cellular concentration.

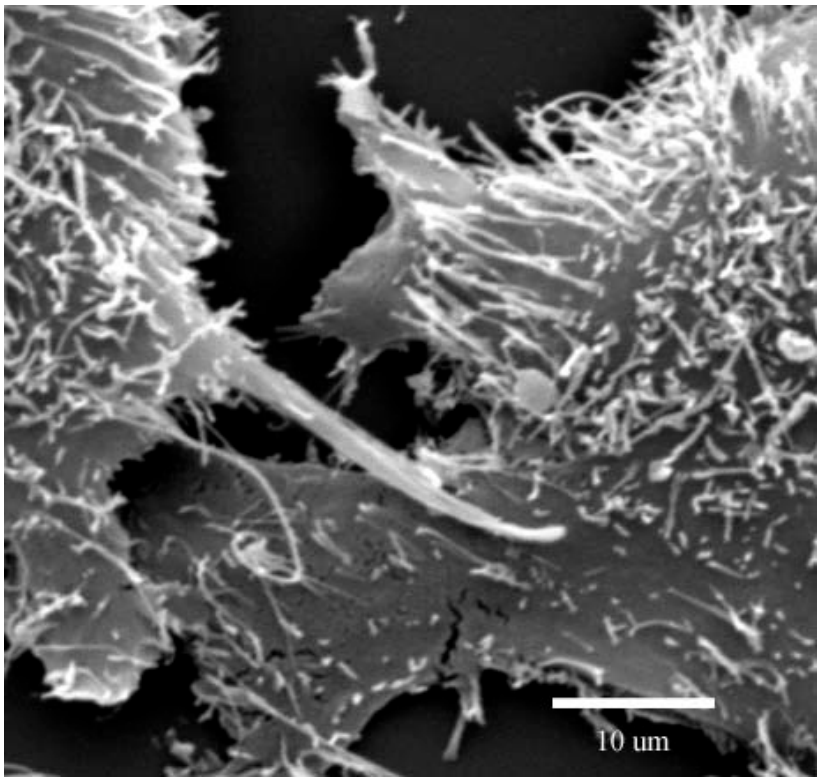
10 um

Figure 29. Thin section showing filopodia along the margin of an MDCK cell.

The oval-shaped objects that look like extracellular material are in fact areas where filopodia are visible. The filopodia are not perfectly flat or straight; in the intact cell, they would bend into and out of this image, which is why only small pieces of the structure can be seen in any one section. The right panel is an exact copy of the left panel, but lines are drawn in to show how the filopodia could have been connected. This aids three-dimensional conceptualization. Scale bar = 500 nm.

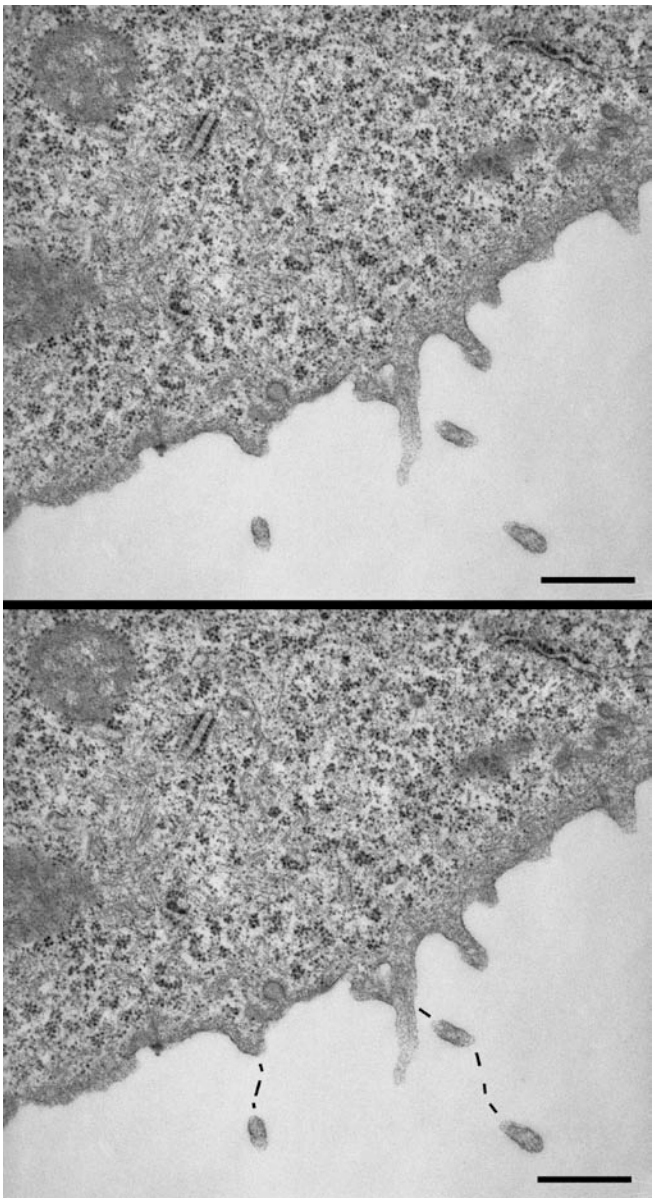

Figure 30. Filopodium with adherent tip.

The filopodium of this detergent-extracted HeLa cell has anchored to the coverslip and appears to be starting to spread laterally into a lamellipodium. Parallel cytoskeletal fibers can be seen diverging as the tip fans out. Scale bar = 10 µm.

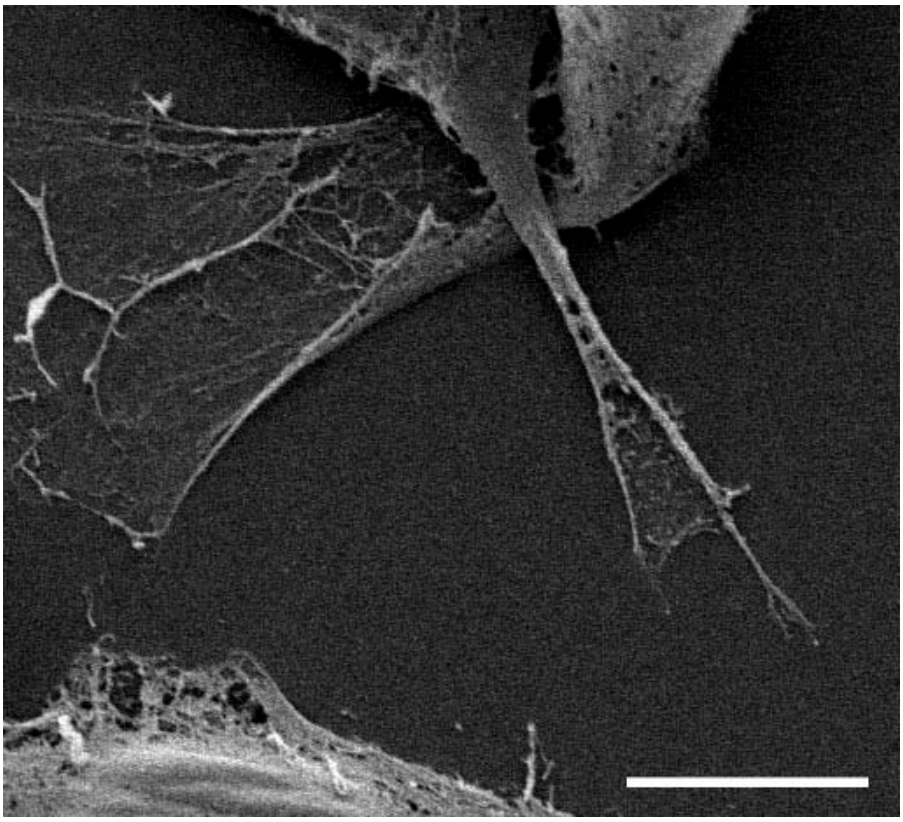

Actin is present throughout the cytoplasm of a cell. However, the allocation and distribution of highly-concentrated actin within the cell seems to vary across cell types. The highest actin concentration in HeLa cells tends to occur at the cell periphery, though thick stress fibers are also observed across the entire cell **(Fig. 35)**. Keratocytes, on the other hand, have a dense concentration of actin around the main cell body **(Fig. 36)**.

The actin content of lamellipodia is heavily concentrated at the very front edge. Both keratocytes and HeLa cells display a dense actin concentration at this location **(Fig. 37)**. In the scanning electron micrographs taken during this investigation, it is difficult to guarantee that the cytoskeletal fibers observed in an extracted cell are actin polymers as opposed to intermediate filaments. However, front-edge fibers observed at high magnification (5,000x – 15,000x) do form a web-like network **(Fig. 38)**, and appear to have numerous short strands at the very front which, if better-resolved and imaged at an even higher magnification, could fit the platinum replica EM results of Svitkina 2007. These findings make it likely that they are, in fact, microfilaments.

The results of this study support current knowledge of the importance of actin in cell motility. Actin fluoresces brightly in filopodia and lamellipodia, particularly at the very front edge. The presence of large stress fibers indicates that actin is also a major structural component of the main cell body.

Figure 31. TEM showing parallel actin microfilament bundles in an MDCK filopodium.

The microfilaments in this filopodium are arrayed in the classic parallel bundle arrangement. Areas where they are especially visible are indicated by arrows.

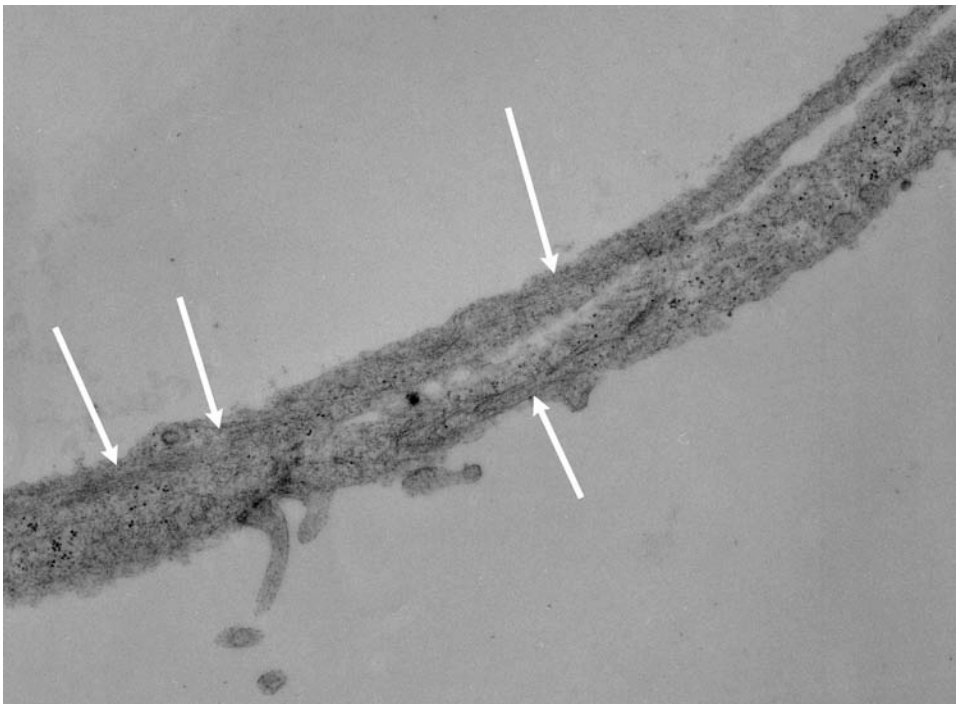

Figure 32. Non-parallel actin microfilaments in a filopodium of a migrating HeLa cell.

The longitudinal microfilaments in this fluorescent filopodium are not completely parallel. The brightest actin filaments in the filopodium are arrayed in the same general direction as presumed motility (indicated by the arrow), but are of both varying lengths and slightly varying angles relative to the overall path of migration. Also, the tip of the filopodium is splayed laterally instead of showing straight, evenly spaced filaments that culminate in a tip that is the same size or smaller than the base of the structure. Instead, the tip of this filopodium is slightly spread, indicating focal adhesions and possible lamellipodia formation at the very initial stages of crawling. Scale bar = 10 μm.

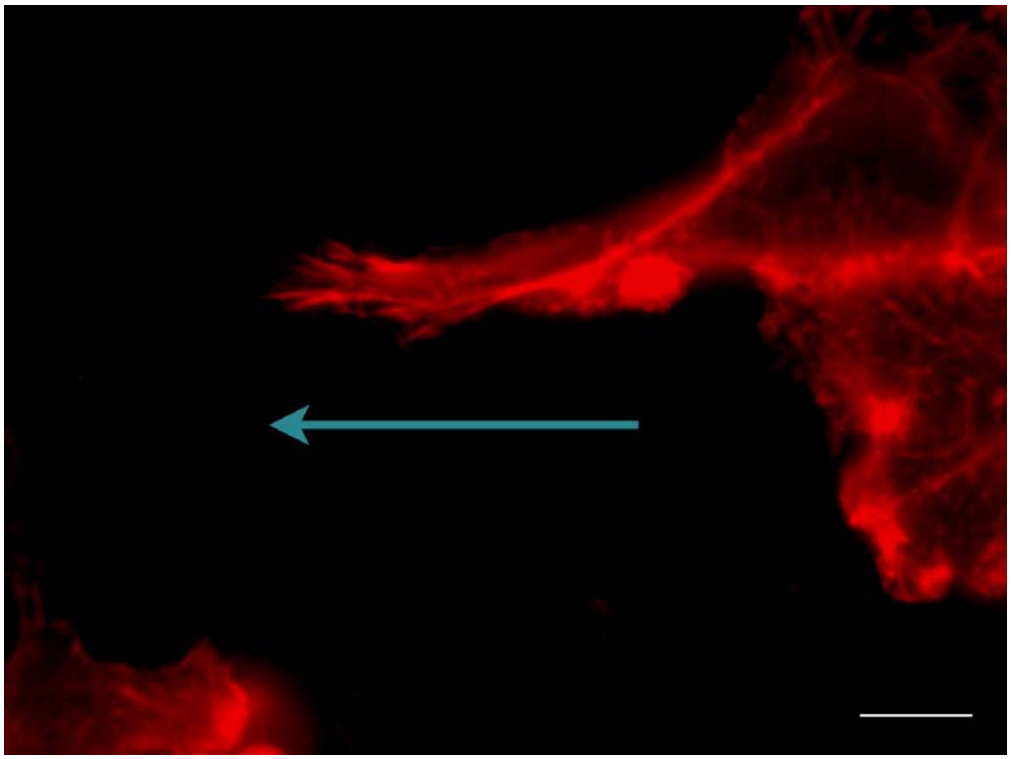

Figure 33. Filopodia beginning to emerge into an empty space.

Wounds made in the monolayer a few hours before staining left gaps into which HeLa cells, like the one seen here, began to migrate. Here, two emerging filopodia are visible protruding into the wound area. Scale bar = 10 µm.

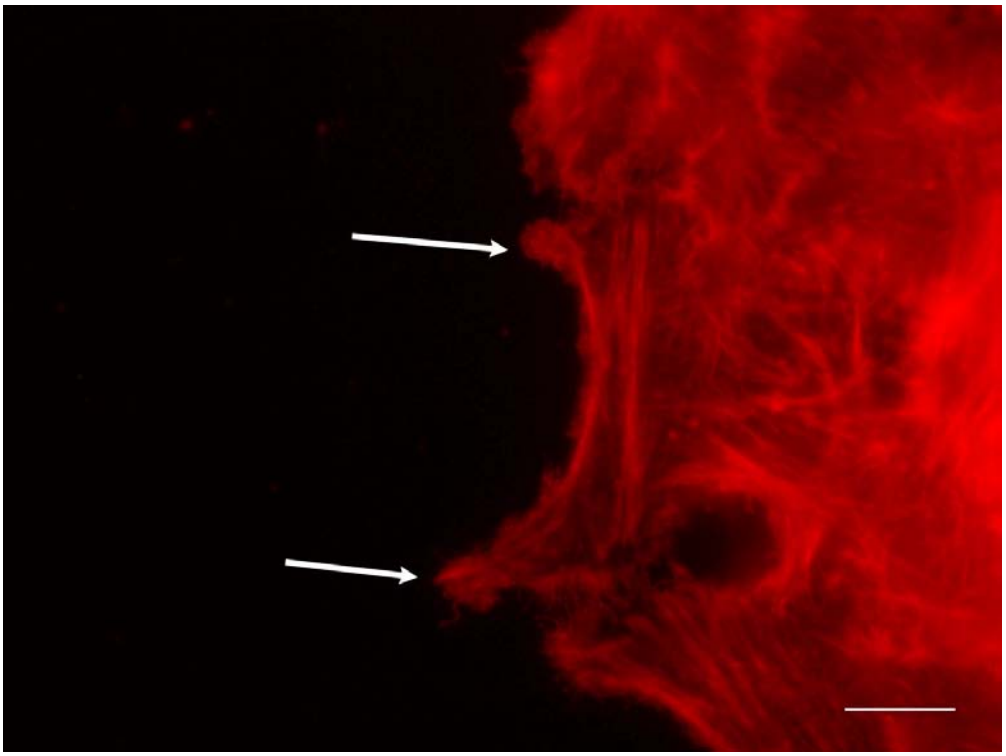

Figure 34. Filopodia are abnormally prevalent in bone-derived mesenchymal stem cells of mice with a mutation on the NPC1 gene.

The mutation, characterized by a limited ability of cells to traffic intracellular cholesterol, may result in mesenchymal stem cells having reduced motility. These cells seem to have small or absent lamellipodia and a larger number of filopodia. The tissue of origin for the cells in this figure was bone marrow, but similar findings are observed in compact bone mesenchymal stem cells from NPC1 mice. Scale bar = 20 μm.

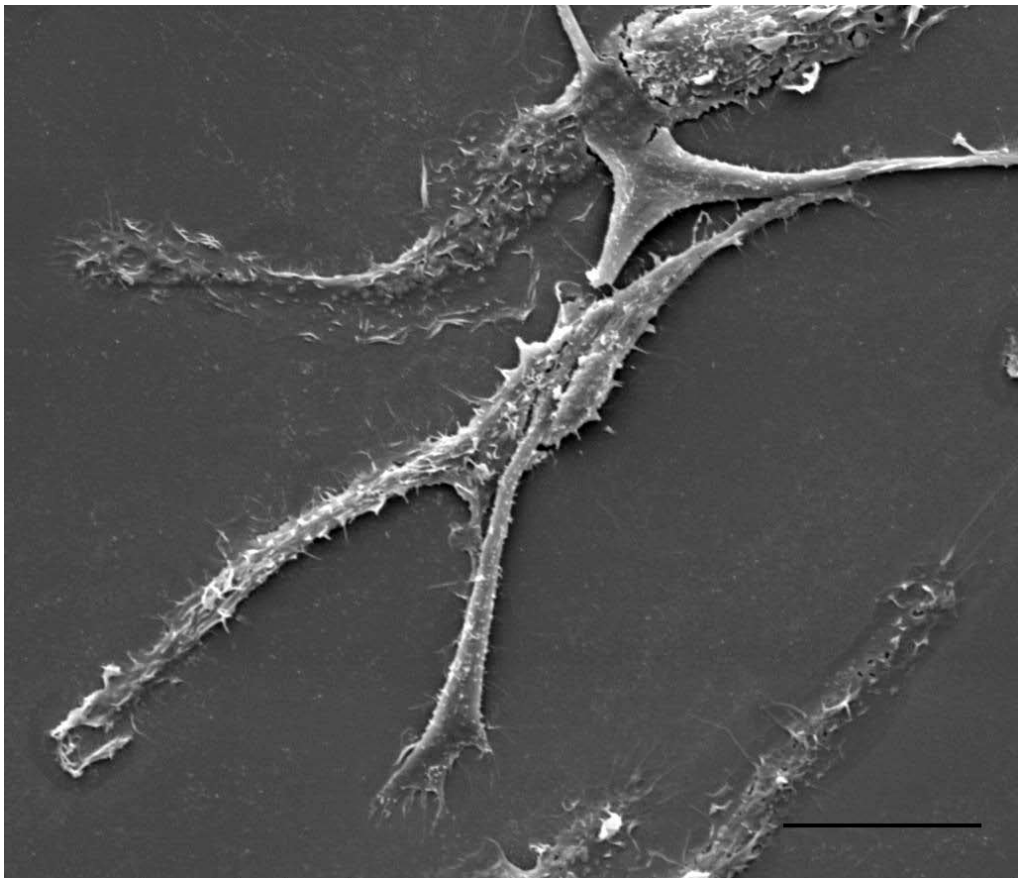

Figure 35. Actin distribution in a fluorescent HeLa cell.

Long, bright stress fibers are the most conspicuous structures in this rhodamine-phalloidin-stained HeLa cell. The transition between the main cell body region and the lamellipodia region is discernible because the thickness of the actin changes; finer filaments instead of thick stress fibers are observed. The fluorescent glow gets brighter again at the very edges of the cell, indicating an increase in actin concentration. The thin actin-containing projections emerging from the lamellipodium are very small filopodia. Scale bar = 10 μm.

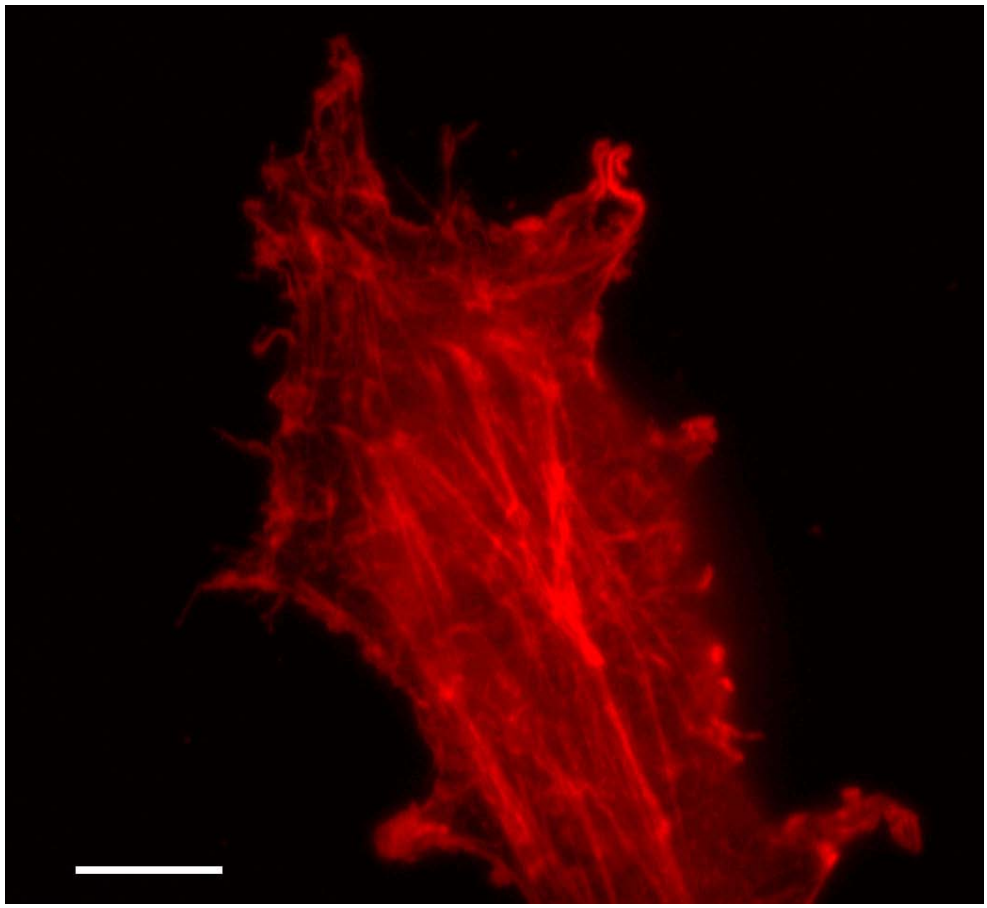

Figure 36. Fluorescent keratocyte showing high actin density around the main cell body.

This crawling keratocyte has a cell body which rises much higher off the coverslip than its lamellipodium. This makes it appear as though the actin concentration is much greater there. The perception is skewed by the thickness differential, but the amount of fluorescence generated by the main cell body is so high in this and in other fluorescent keratocytes that it is possible to conclude a different pattern of actin distribution than observed in HeLa cells. Scale bar = 10 µm.

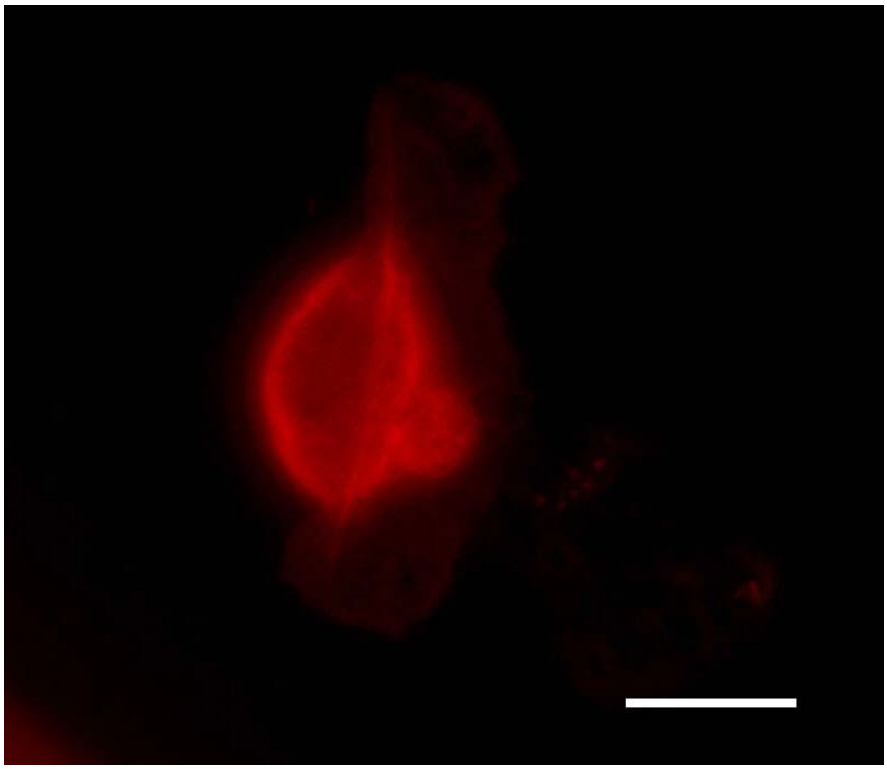

Figure 37. Dense actin concentration at the very front edge of emerging lamellipodia.

The HeLa cells in the top panel have thin areas of bright actin staining at the margin of the leading edge, as do the keratocytes in the bottom panel. This supports the idea of many branched, concentrated microfilaments at that location within the cell. Scale bar = 10 µm.

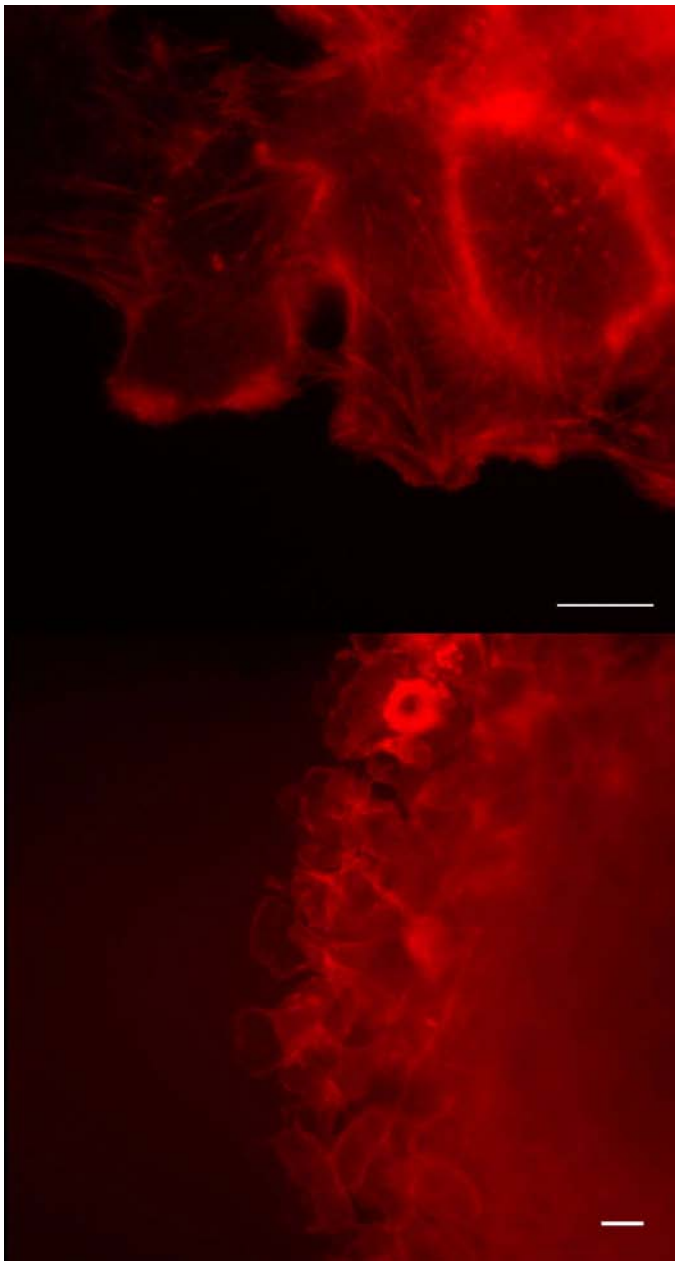

Figure 38. Network of cytoskeletal fibers in an extracted HeLa cell under SEM.

In this high-magnification image of a HeLa cell with plasma membrane removed by detergent treatment, it is probable that the dense cytoskeletal fibers observed are microfilaments. Microfilaments are more likely than intermediate filaments to be present near the leading edge of a lamellipodium, and they also form finer branching patterns than intermediate filaments. Scale bar = 2 μm.

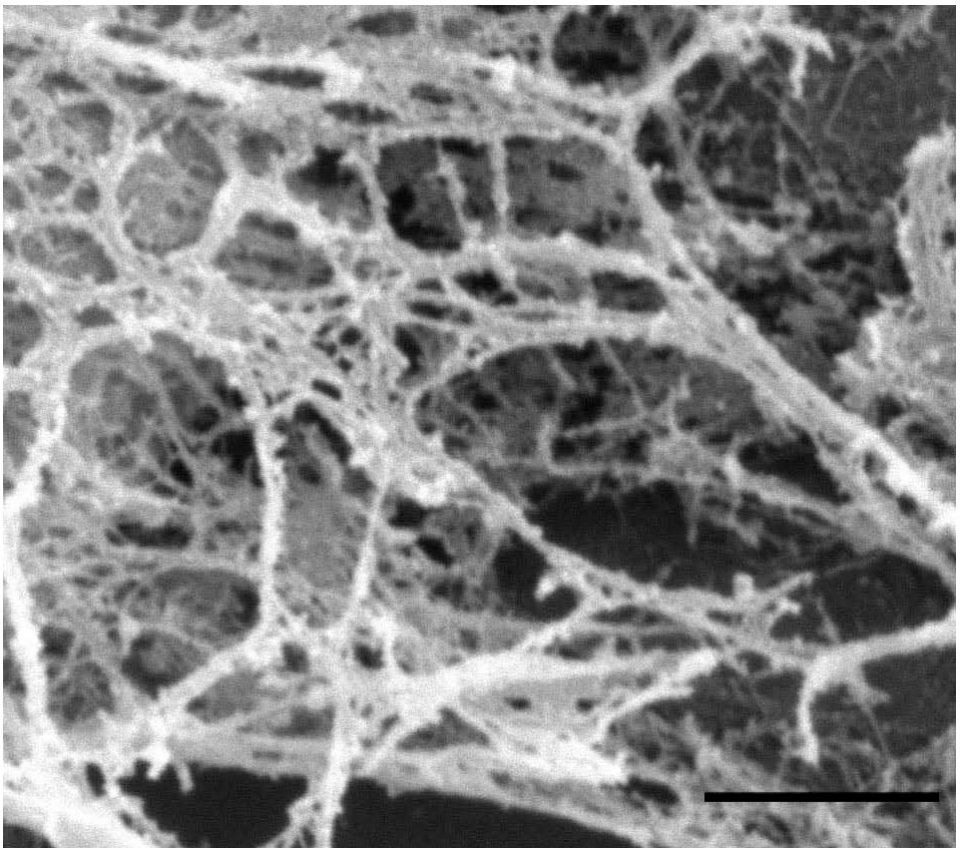

Figure 39. TEM showing many microfilaments at the margin of an MDCK lamellipodium.

The microfilaments in this micrograph vary in length, from the longer fibers that run parallel to the cell margin to the much shorter microfilaments at the very edges of the cell that appear to branch and criss-cross. The former are transverse arcs, while the latter are most likely branched Arp2/3 microfilaments. Scale bar = 500 nm.

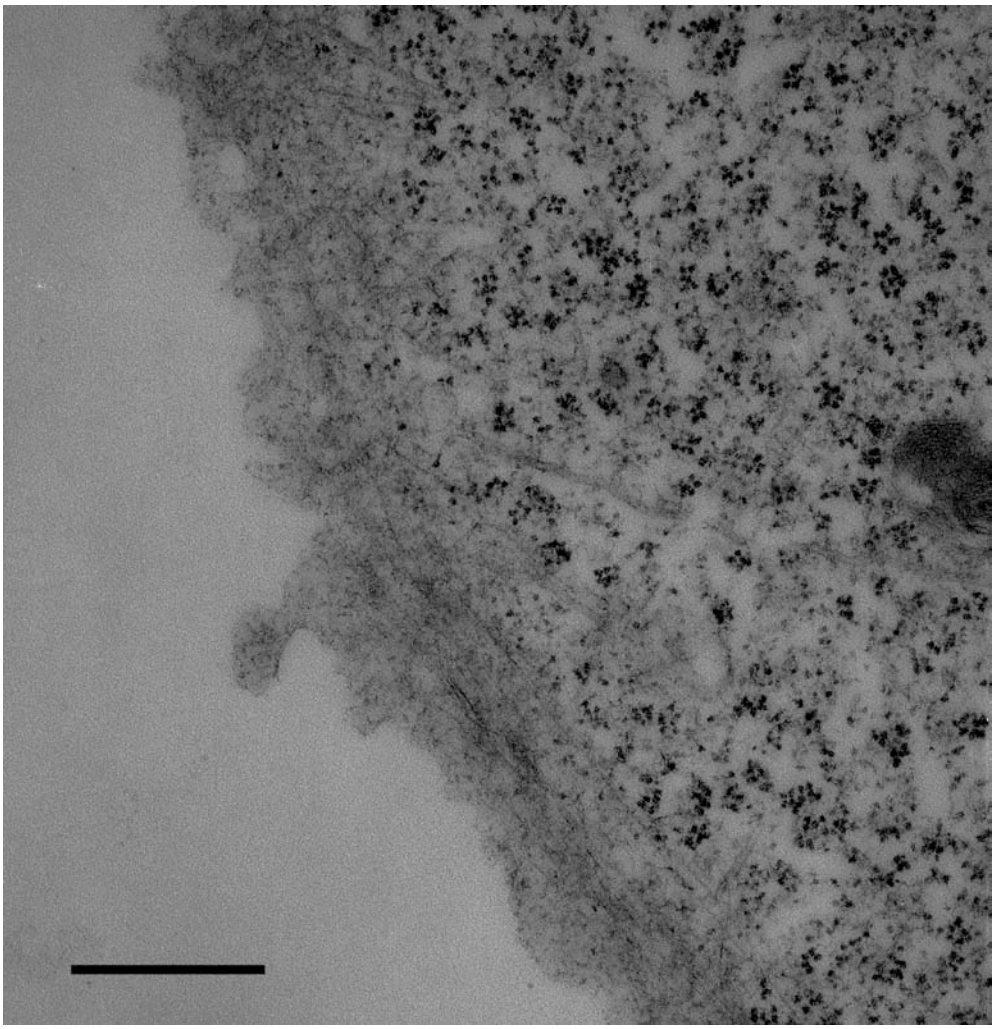

DISCUSSION

The significance of the morphology of migratory cells

The determinative relationship of form to function holds true in migrating cells. The internal, branched actin structure of a lamellipodium increases the area of contact and the number of contact points with which to push the plasma membrane forward. Bundling of long microfilaments in filopodia, on the other hand, stabilizes them as they lengthen forward against a much smaller area of the membrane that lies perpendicular to the direction of extension.

Stress fibers are usually quite thick and prominent. They maintain traction against the substrate as the cytoplasm contracts; tensile force must be constantly balanced between the growing end of the stress fiber and the focal adhesion at the other end (Alexandrova 2008). This is why they glow so brightly under fluorescence, and why they are also very noticeable under SEM and TEM **(Fig. 40)**.

In the cell types examined in this study, actin is clearly required for cell locomotion. Most migratory cell types, with very few exceptions, use actin to crawl along a substrate. The importance of actin in motility is highlighted by certain observed phenomena. For instance, a filopodium cannot form without actin microfilaments to stabilize and drive the protrusion, but the actin *can* depolymerize to leave behind an adherent, membrane-bound extension in the shape of the filopodium (though it can no longer grow) (Yang et al. 2009). Also,

lamellipodia are sites of high actin polymerization and recycling activity, which is related to the dense actin concentration observed under fluorescence at the leading edge.

The three-dimensional structure of filopodia, like that of other cellular structures, is difficult to visualize using TEM. However, once oriented to the objects being viewed in cross-section, the observer can gain an enormous amount of information about them. For instance, what look like vesicles outside the plasma membrane are, in fact, portions of filopodia. Some of them belong to the same, curving filopodium that goes out of the plane of the section and then reappears nanometers away **(Fig. 29)**.

The observance of more filopodia in NPC1 mice vs. wild type mice may be related to the inability of the bone-derived MSCs to form lamellipodia. The NPC1 mutation affects one of two genes responsible for encoding proteins that work together to traffic cholesterol out of the late endosome. Problems with endolysosomal lipid vesicular trafficking affect plasma membrane microviscosity (Vasanji et al. 2004), actin polymerization (Theriot 2000), and the movement of important actin cross-linking activator molecules such as Syndecan-1 that depend on these “lipid rafts” to get to the microfilaments at the leading edge (Chrakravarti et al. 2005). Actin cross-linking is vital to lamellipodia formation. In the absence of cross-linking agents, microfilaments may organize instead into the parallel arrays found in filopodia, making filopodia far more abundant (Mejillano et al. 2004). This is a possible reason for the abnormally large number

Figure 40. TEM showing the network of stress fibers inside an MDCK cell.

This micrograph shows the orientation and distribution of stress fibers within a crawling epithelial cell. The thick stress fibers are made of large bundles of actin microfilaments. They help support the structure of the cell against all of the forces involved in cell motility, and typically grow from focal adhesions. Scale bar = 2 μm.

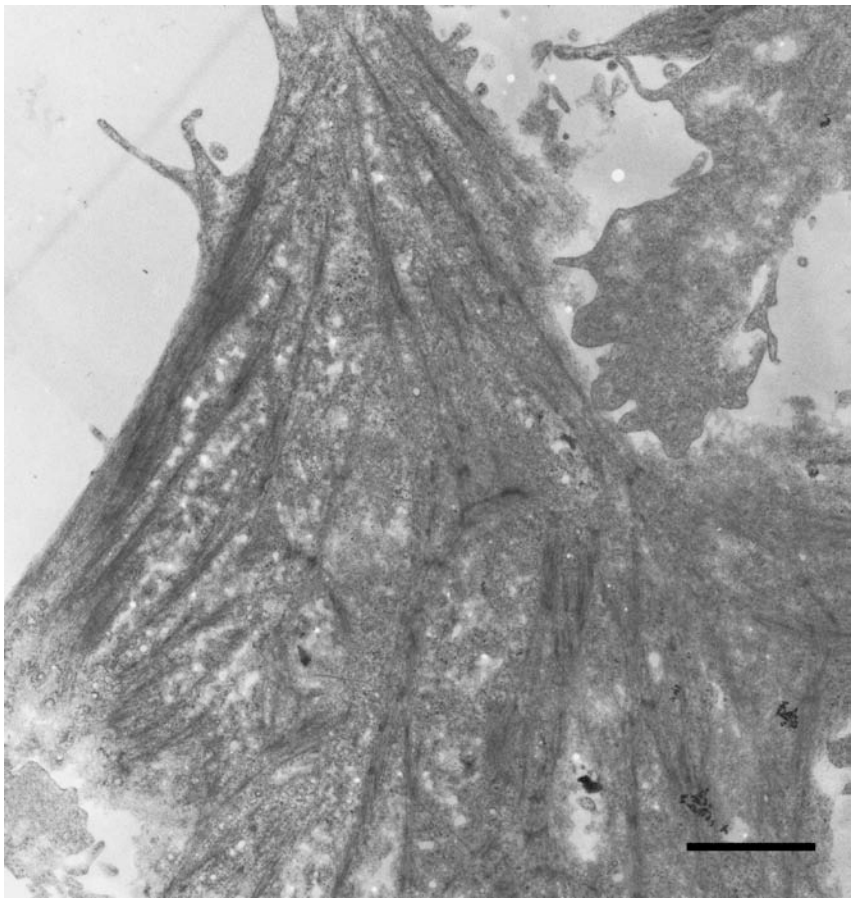

of filopodia and the apparent lack or gross reduction of lamellipodia in NPC1 adult mouse mesenchymal stem cells.

The NPC1 mutation and the disease associated with it highlight the extreme, though not well-studied, importance of mesenchymal stem cell migration in vivo. Cell migration is a valuable property in general; all migratory cell types crawl for a reason. Whether it pertains to stem cells, fibroblasts, or tumor cells, cell migration research is widely applicable. Findings of such studies can have implications in a variety of scientific fields, particularly in the area of medicine.

Applicability of cell motility studies

One of the most active areas of medical research is oncology, the study of cancer. Cell migration comes into play during metastasis, when cancer cells migrate outside the tissue of origin and invade other tissues. Normally, tumor cells such as HeLa keep dividing beyond confluence; if there are any gaps between cells, mitotic divisions will quickly fill them in. HeLa cells are also motile and can crawl in groups into empty regions **(Fig. 2)**. Therefore, they not only grow and proliferate, but also migrate.

Cancer cells are not the only migratory cell types associated with a tumor. When a tumor becomes malignant, it sends out paracrine signals such as VEGF (vascular endothelial growth factor) to induce vascular endothelial cells to move in and form new blood vessels, which supply the tumor with oxygen, nutrients, and waste removal (Bauer et al. 2007). The hypoxic conditions under which

tumors grow prior to vascularization are known to trigger the release of diffusible angiogenesis-promoting signals. The signaling pathways involved with endothelial response to VEGF and other molecules are complex, but once the endothelial cells transduce the original signal, a cascade of events takes place. Blood vessels become permeable and the endothelial cells that comprise them are loosened via proteases. This allows the cells to migrate into the stroma, which is the ECM-rich extravascular connective tissue, and from there to the growing tumor. Along the way, endothelial cells secrete proteases to degrade certain ECM fibers, an activity which creates adhesive gradients in the stroma. The paths of other endothelial cells are directed (via haptotaxis) by these gradients (Bauer et al. 2007). As a consequence of these events, oncological research is especially interested in the mechanics of endothelial cell migration in response to tumor growth.

Another active area of study is wound healing and regeneration; here, cell migration plays a large role. Cutaneous injuries spur an immediate and large-scale response from hematopoietic, mesenchymal, epidermal, and endothelial cells. First, a clot is formed by platelets; this clot not only stems blood loss but also provides a dense and intricate substrate for migratory neutrophils, macrophages, and fibroblasts. Immune cells cleanse the wound area and destroy pathogens while fibroblasts enrich the extracellular matrix so it can sustain epidermal growth, repair, and formation of new blood vessels. Of all the cell types involved in wound repair, fibroblasts seem to be the limiting factor slowing repair (Singer

and Clark 1999). Though faster than many collectively-migrating cells, fibroblasts are considered relatively slow among individually-migrating cells (Alexandrova et al 2008). Not only do they produce fibronectin, collagen, and other ECM components, but they are responsible for organizing these materials as well. The ECM must provide exactly the right environment for other processes, many of which also involve cell crawling. These processes include endothelial sheet migration, neovascularizton, and eventually, muscle restoration. Fibroblasts, therefore, must be recruited quickly from the surrounding tissue. Having too few fibroblasts delays wound healing, while too many indicates over-proliferation and/or abnormal cell migration, and results in scarring (Singer and Clark 1999). Cell migration, particularly in the context of cell-substrate interactions, is crucial to proper wound healing.

Many cells of the immune system are able to migrate rapidly. White blood cells, such as leukocytes, monocytes, and mature macrophages, are able to move from blood vessels into the stroma through diapedesis. Also called extravasation, diapedesis is done in response to tissue infection or injury. A commonly studied model for cellular motility, T cells move at an average rate of approximately 6-8 μm/min. on coverslips. Neutrophils move even faster, averaging 8-16 μm/min (Friedl et al. 2001). Cell motility studies may help to illuminate the means by which immune cells are able to travel to target destinations during the immune response.

Immune cell migration is also observed in the lymph nodes. These glands,

which are sites of T, B, and other immune cell propagation, are specially compartmentalized. Cells segregate by type, necessitating migration within lymph nodes (Bajénoff et al. 2006). Reasons and mechanisms for this type of migration are still largely unknown.

Though all of these cases involve cell migration in vivo, studies using cultured cells may be applied to all. In vitro motility studies have been and continue to be extremely useful. Growing cells on coverslips makes them easy to image, and carefully controlling exactly what goes into the culture dish limits environmental variability. Also, cells grown on coverslips make good models for the effects of various chemical treatments. New techniques of imaging in vivo will only add to the richness of available methods; in vitro studies will not soon die out.

Live imaging of cells both in vitro and in vivo is one of the most useful tools a microscopist has at her disposal. Still images can reveal various aspects of cell migration, but videos of crawling cells capture and convey the whole process. If a picture is worth a thousand words, a video is worth at least ten thousand; it shows, from beginning to end, exactly what all of the pictures cooperatively describe. Live imaging is one of the many branches of microscopy where new technology and procedures have made it possible to see motile cells as never before.

Alternative techniques in microscopy

The field of cellular and tissue microscopy has made extraordinary leaps in the past few years. New ways to obtain, capture, and adjust images to extract the clearest and most pertinent information are constantly being honed through advanced technology. From microscopes to cameras to computer software, tools for studying smaller and smaller objects are revolutionizing biology. Some examples are described later.

First, however, it is worthwhile to point out some alternatives amongst well-established techniques. In the field of fluorescence microscopy, confocal microscopes – which have been in use since the 1980s – are able to construct sharp, three-dimensional images of relatively thick cells. The technique of laser scanning at different focal planes, and compiling these scans into a 3D image, overcomes some of the limitations of traditional fluorescence microscopy. In regular fluorescence microscopy **(Fig. 41)**, out-of-focus regions appear to glow more brightly than those that are in focus, so – though it is possible to extrapolate an approximate concept of how deep these regions lie with respect to one another – neither the quality nor the precision equates to that of confocal micrographs.

A similar comparison can be made between traditional phase/contrast microscopy and differential interference contrast (DIC) microscopy **(Fig. 42)**. DIC uses polarized light to generate two offset images of the sample, which both constructively and destructively interfere with one another at different areas, creating contrast. Like human stereo vision, which occurs because the eyes see the

world at two slightly different angles, the offset produced by the DIC beam-splitting prisms forms a 3D image. DIC enables objects at different focal planes to be in focus simultaneously, which regular phase/contrast microscopy does not allow. Furthermore, there are fewer artifacts in the final image than there are under phase.

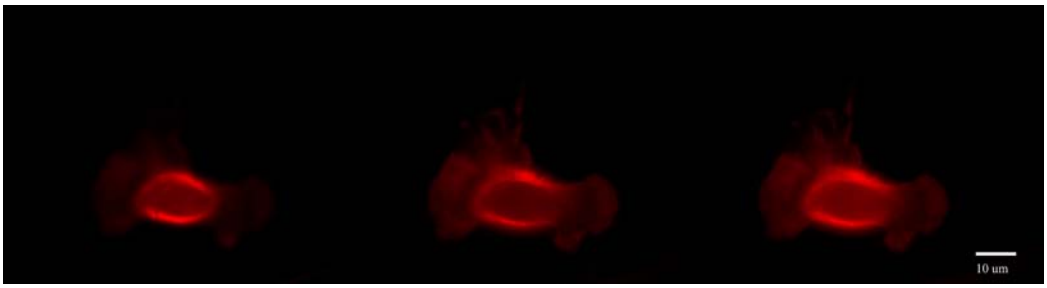

Figure 41. Cellular regions that are out of focus fluoresce with an exaggerated size and intensity, as observed in a fluorescent keratocyte captured at three different focal planes.

This figure displays three images of the same, fluorescent keratocyte taken at slightly different focal planes. In the first image, the main cell body is more in focus than the lamellipodium; the actin network fluoresces as a bright ring encasing the main cell body. This ring will never be entirely in focus, because the main cell body of a keratocyte rises so high off the coverslip that the majority of microfilaments surrounding it are always out of focus. This is especially true when the flat lamellipodium is more in focus, as it is in the right-most image. While distinct microfilaments of the lamellipodium are discernible in this panel, the ring of actin encasing the main cell body appears thickest and blurriest here - indicating that it is completely out of focus. The left-most image focuses on the top portion of the cell; the center image, a little lower; and the right-most image focuses on the bottom portion of the cell which includes the lamellipodium. Scale bar = 10 μm.

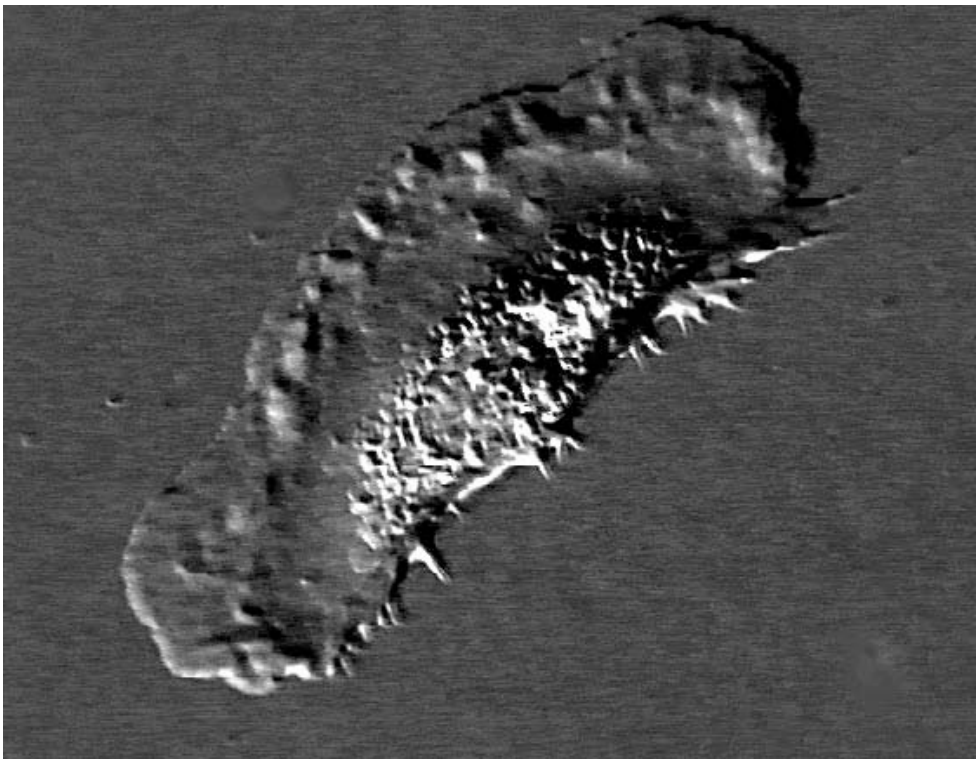

Figure 42. Goldfish epidermal keratocyte under DIC microscopy.

This keratocyte image, captured by Dr. Mark Cooper of the University of Washington, appears three-dimensional. Membrane ruffles are visible as raised, mogul-like structures on the leading edge, while the main cell body seems to have many small surface protrusions. Several thick retraction fibers are also visible on the trailing edge of this cell.

Techniques at the cutting edge of microscopy include photoactivated localization microscopy (PALM) and its more recent off-shoot, interferometric photoactivated localization microscopy (iPALM). These involve photoswitchable fluorescent molecules tagged onto proteins of interest. The fluorophores are excited to fluoresce by brief exposure to a strong beam of light at a certain

wavelength, but only some of these tags will activate during any one exposure. When they photobleach, another round of photoactivation causes a different distribution of molecules to fluoresce. The information is gathered, layer by layer, as bright, discrete dots instead of a smear of unresolvable fluorescent data. It allows researchers to pinpoint single molecules using software that applies Gaussian analysis to the point-spread function (PSF) of any one fluorescent event, finding peaks that indicate the location of the centers of these events – which is most likely to be the precise location of a single, tagged molecule of interest. This far exceeds the capability of a normal fluorescent microscope, which is constrained by the 200 nm resolution limit for a beam of photons. iPALM takes the method a step further by introducing simultaneous multiphase detection of single photons that self-interfere when they encounter a 3-way beam splitter, allowing localization of the z-axis coordinate. Therefore, PALM resolves x-y molecular specificity while iPALM forms a three-dimensional view of the sample (Shtengel et al. 2009).

Finally, freeze-fracture replica immunolabeling (FRIL) electron microscopy similarly enables three-dimensional visualization of the internal components of a cell, but here it is the distribution of heavy metal immunolabels super-imposed onto the platinum-carbon replica-generated image that show where specific, tagged molecules existed. The freeze-fracturing technique for electron microscopy not only allows for extremely rapid fixation – which correlates with more accurate, true-to-life results – but also causes the cell to splinter in layers

between the two lipid monolayers of the plasma membrane. Evaporation of platinum onto the specimen, and subsequent decay of living tissue, leaves three-dimensional surface impressions of both sides of each monolayer and their associated proteins (Robenek and Severs 2008).

Any and all of these techniques can be (and some have been) applied to the cell types in this study. Enormous amounts of information can be gained from these high-powered tools. For example, Schroff et al. published results in 2008 using focal adhesions as a model for demonstrating the applicability of PALM. PALM was able to resolve the distribution, precise localization, and density of tagged adhesion proteins (Schroff et al. 2008). Dr. Svitkina routinely uses platina replica EM to image Arp2/3 actin at the leading edge of lamellipodia in fish epidermal keratocytes **(Fig. 6)** (Svitkina 2007). With many technological options, and even more cell types to explore, the possibilities for imaging the cellular and extracellular materials involved in cell locomotion are plentiful.

The value of imaging

But why image? Molecular characterization, flow cytometry, genetic sequencing, biochemical assays, and experiments involving computational models can provide solid, quantitative data to work with. Microscopy, however, is a powerful tool whose importance cannot be overstated, particularly when used in conjunction with or put into context of other forms of biological research.

Through visual data, cell microscopy reveals physical facts about the smallest independently-functional units of life. Perhaps one of the biggest draws

to cellular imaging is that, unlike other forms of data collection at the cellular and molecular level, the results are visually displayed in the context of a photograph of the studied phenomena. This is also part of microscopy's major challenge: how can visual, qualitative information be quantified, and how can its interpretation be validated? Only through countless studies – work that layers in new information while using and re-framing prior understanding – can a library of image-based knowledge be constructed.

Besides the obvious yield – photographs of cells and cell structures – there are numerous tasks that can be accomplished using a microscope. Immunolabeling using fluorescent or heavy-metal-tagged antibodies (depending on the type of microscopy) shows the distribution, density, and location of molecules of interest. Electron tomography uses images of serial thin sections to create a three-dimensional model of cell structures, which are normally viewed in cross-section on two-dimensional photographs of a single slice. SEM backscatter images compare material densities across different regions of the cell, while energy-dispersive x-ray spectroscopy (EDS) uses an x-ray detector to record the exact elemental make-up of a sample. Compound light microscopy of tissue sections shows intercellular organization, while fluorescent cellular markers reveal the presence and location of specific cell types within the tissue.

In this study, five types of microscopy were used to form an overall understanding of the migration of five different cell types. Often one type of imaging confirmed results seen under another form of microscopy. For instance,

the distribution and appearance of stress fibers seen under fluorescence **(Fig. 3)** looks remarkably like the pattern observed under TEM **(Fig. 40)**. In other cases, information from one kind of image expanded the knowledge gained from another. For instance, the raised, leading edge ruffles seen under SEM **(Fig. 23)** provide a detailed – though static – glimpse of the dynamic, wave-like surface motion seen in the time-lapse videos **(Movie 1)**. In this case, the capabilities of one type of microscopy overcome the limitations of the other.

In addition to the actual microscopy, there are other factors which contribute to both the quality of the image and the accuracy of the information that can be extracted.

The experimental process: preparing and imaging motile cells

Since the essence of this study is partially focused on the methodological approach, and not just on the results themselves, it is important to discuss attempts, failures, corrections, and successes during the process of preparing and imaging motile cells.

As alluded to in the results, insight is often gained when the experimental procedure yields inaccurate results or no results at all. Poor preparation can change both the amount and the accuracy of data collected from microscopic images, producing misleading results that include morphologies, artifacts, and phenomena that did not reflect the cells' true or natural state. Results are questioned when compared against micrographs which both literature and laboratory observations suggest to be more acceptable. When the problem lies in

the protocol itself (i.e. there is no human error), the process then becomes an investigation to find the step in question and then to correct it. This research is critical to the process as a whole. Pinpointing the problem is the first step, but the problem must then be corrected. Some examples of preparations that went wrong are discussed in the following sections, along with corrections that made a significant difference.

Contamination is a common issue encountered when culturing cells. Stem cells are particularly sensitive to any bacterial or fungal contaminants in their culture. Even when sterile procedures are strictly followed, the medium sometimes becomes infected with microbial invaders. Fungus not only affects cell health, but also interferes with imaging **(Fig. 43)**. Furthermore, to an observer not involved in the culture of the cells in question, fungal growth could be potentially mistaken for a structural trait of the cells themselves. There are many different kinds of fungal contaminants that assume a variety of shapes, and when the whole culture is infected, it is sometimes difficult to ascertain what is a) cell material; b) fungus; or c) abnormal cell material secreted in response to the infection.

Cell concentration is another consideration when culturing cells for microscopy. Plating cells on coverslips involves balancing existing cell concentration against the expected time window during which the cells will be allowed to grow and populate. An ideal threshold must be achieved. Below that ideal concentration, cells will be too sparse. Their health (and consequently their morphology) will be different than at the ideal concentration, and any attrition

suffered by the population during treatment and/or fixation may result in a dearth of available material to image. Conversely, when cells are seeded too heavily, neighboring cells may contaminate each other with accumulating cellular waste. Stem cells, which migrate as individuals but populate a culture substrate as a monolayer, seem to require the presence of neighboring cells but not excessive physical contact with them. Spherical cells with decreased adherence and many small surface protrusions are evidence of a coverslip that is too crowded with cells **(Fig. 44)**. This is a phenomenon observed in both stem cell and HeLa cell cultures. **Figure 15** provides a good example of a stem cell colony at the right cellular concentration.

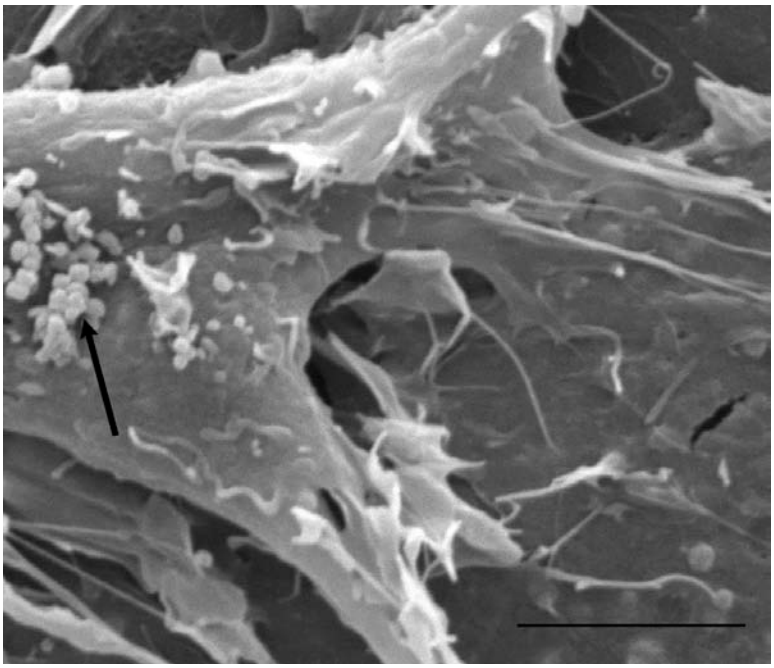

Figure 43. Fungal contamination of a stem cell culture. Scale bar = 5 µm.

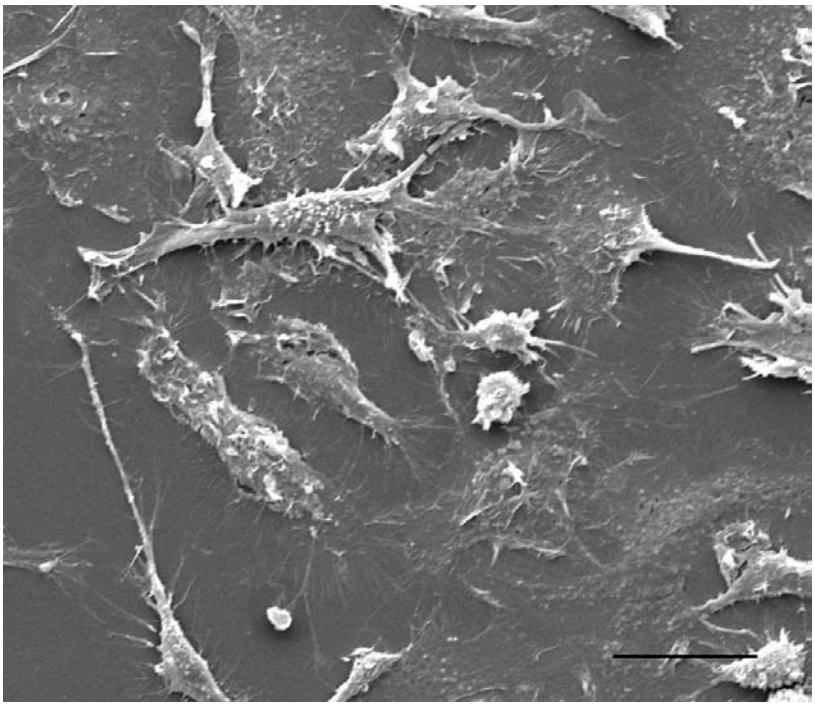

Figure 44. Overgrown stem cells under SEM.

Ideal cellular concentration depends on the cell type. HeLa and MDCK cells, for instance, form fully confluent monolayers while remaining healthy if not allowed to overgrow. Stem cells, however, seem to be more sensitive to crowding and need a certain amount of space between neighboring cells. In this image there are some spherical, non-adherent cells that most likely died before the sample was fixed. The cells that are adherent display a normal overall shape, but the abundance of surface protrusions and many retraction fibers indicates that they are under environmental stress due to overcrowding. Scale bar = 25 µm.

Finally, the ingredients of the culture medium can strongly affect whether or not cells will survive, proliferate, and/or migrate. The keratocyte culture medium, as described in the methods and materials section, contains 90% Liebovitz's L-15 culture medium and 10% Gibco fetal bovine serum. Previously, a media recipe comprised of the same concentration of L-15 and the same

concentration of a different brand of FBS was used to culture keratocytes, but these cultures were never successful. The cells remained round, suspended in the fluid, non-adherent, and grouped together. When the other brand of FBS – which had worked perfectly well for HeLa culture – was replaced with Gibco FBS, the keratocytes flourished.

Once the culture has been established successfully, cells must be properly prepared for imaging. The experimental question dictates which structures are to be viewed, which in turn determines 1) whether or not the cells should be alive during imaging; 2) the types of chemical treatments the cells must undergo; and 3) whether or not the fixation must be permanent. For instance, some fluorescent samples – though fixed with the quick protein cross-linker formaldehyde and extracted with acetone – are discarded immediately after imaging because the fluorescent stain quickly degrades in a diluted state. Therefore, it is not necessary to treat them with the slower, more permanently stable protein cross-linker glutaraldehyde, which is instead reserved for electron microscopy specimens that, once fixed, can be stored for several years (depending on the sample). The functional difference between formaldehyde and glutaraldehyde is that the first is a rapid but reversible cross-linking agent, while the second is a slower but permanent cross-linker. The first is suitable for disposable preparations while the second is more ideal for samples that can be imaged multiple times.

Another consideration is whether to view the surface or the internal structure of a cell. If the latter case applies, then the plasma membrane needs to be

chemically removed. In the case of TEM, thin-sectioning negates the necessity of extracting the cells because the slices produced are cross-sections, where the membrane does not block internal imaging. However, if internal structures such as cytoskeletal fibers are to be studied under SEM or fluorescence, the plasma membrane must be removed by adding a detergent or acetone solution immediately prior to or immediately following primary fixation. Otherwise, the cell surface and not the interior will be visible.

Membrane extraction can be complicated. HeLa cells treated with a detergent solution lost membrane and cytoplasmic material, but the cytoskeleton and overall cell shape remained reasonably intact and showed similar morphologies to cells observed under phase, fluorescence, and SEM without extraction. This was not the case with keratocytes. In one experiment, SEMs of presumed keratocytes that underwent the extraction procedure revealed cell-like objects with almost no resemblance to non-extracted keratocytes, except for their comparable size. These objects, typically about 30 micrometers in diameter and faintly polygonal, were thick and appeared to have a honeycombed texture **(Fig. 45)**. No lamellipodia, filopodia, or retraction fibers were observed. These cells were unrecognizable and did not match anything in the literature, so if they were indeed keratocytes, they were grossly distorted during the extraction and/or fixation process. Successful plasma membrane extraction of fish epidermal keratocytes using Triton X-100 has been accomplished (Svitkina 2007, fig. 4), and the poorly-fixed cells in this study did not resemble any images of keratocytes

found in the literature.

Care must also be taken when transferring cells from the incubator, where they thrive at optimal temperature and carbon dioxide level, into a rinse buffer and then into primary fixative solution. Mesenchymal stem cells isolated from the bone marrow thrive in slightly hypoxic conditions. When the culture medium or coverslips themselves are exposed to the air for too long, these cells detach, shrivel, and become round instead of flat **(Fig. 46A)**. They either retain pre-existing filopodia or send out new, abnormally long filopodia **(Fig. 46B)**. The images in **Figure 46** were taken using samples that had been left out of the incubator for too long (approximately eight minutes) immediately prior to fixation.

A final case where manipulation of cells prior to microscopy can have adverse effects on cellular vitality is observed in keratocyte culture preparation. *Fundulus* scales are surrounded by a layer of keratocyte-rich tissue which must be dissected from the scales themselves. The pieces of tissue are small but visible to the naked eye, and when viewed on a coverslip even under a low magnification their thickness impedes imaging. They rise so high off the glass that it is impossible to even approach good focus throughout the entire frame. Furthermore, hundreds of cells form this tissue mass, leaving a disproportionately small number exposed along the margins with room to migrate away. This reduces the number of adherent and potentially photographable keratocytes; Therefore, mechanical or chemical separation of the tissue clumps prior to plating

is an attractive idea, and was attempted using physical agitation as well as a trypsin/EDTA digestive solution.

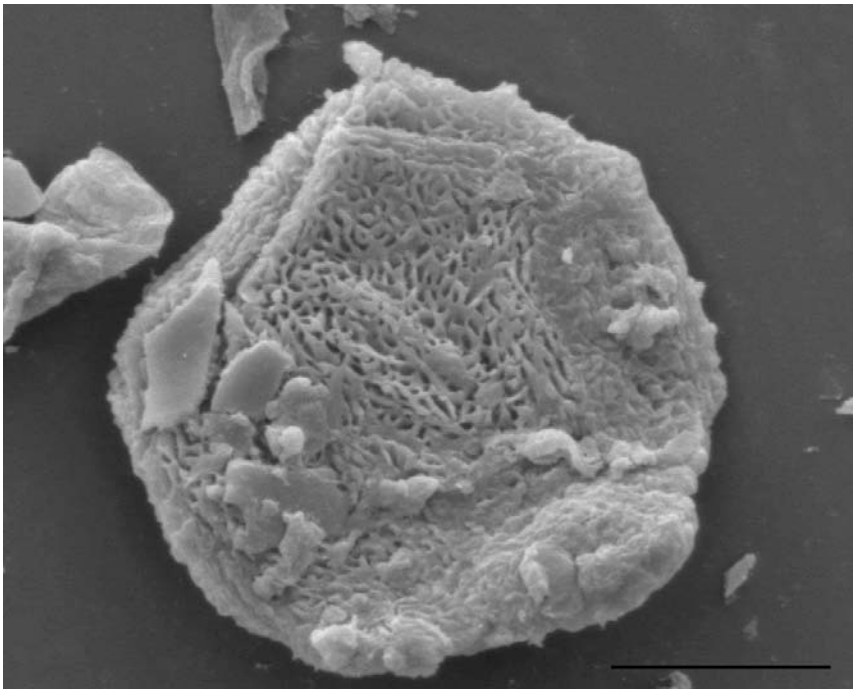

Figure 45. A cell thought to be a keratocyte distorted by detergent extraction. Scale bar = 10 µm.

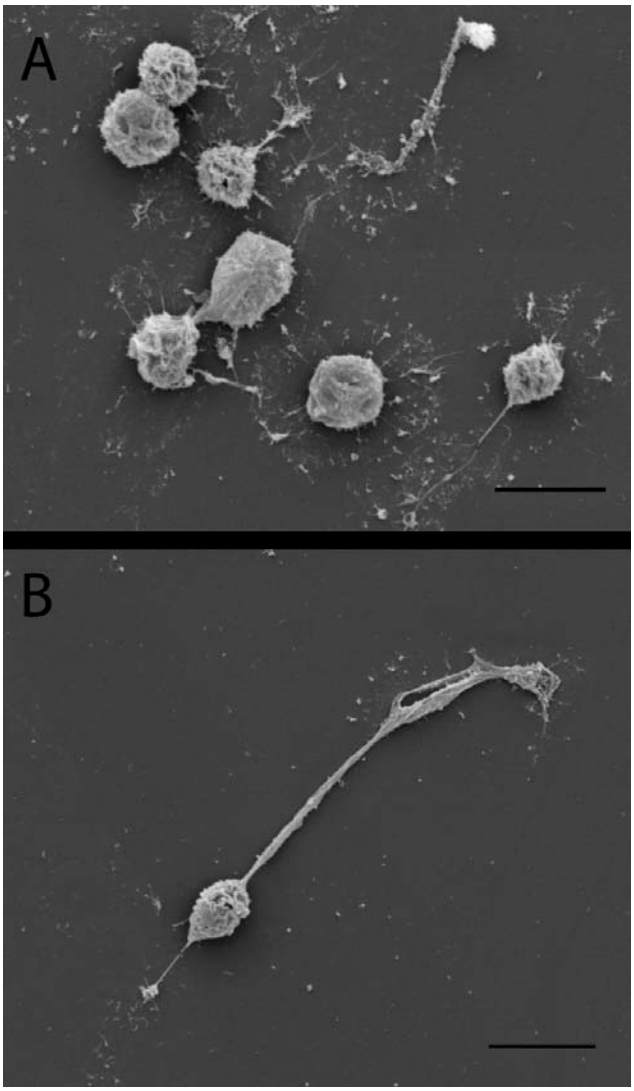

Figure 46. Mouse compact bone mesenchymal stem cells exposed to too much oxygen immediately prior to fixation.

Both panels in this figure were imaged from the same coverslip. In addition to a long filopodium, which may have been sent out in response to the sudden inundation with atmospheric levels of oxygen, the cell in panel B – like those in panel A – has a rounded-up, unhealthy appearance. Scale bar = 20 μm.

Gross mechanical separation using repeated pipeting and shaking resulted in larger tissue clumps with fewer, but healthier, cells **(Fig. 47B)**. Comparatively, chemical separation using a trypsin/EDTA digestive solution resulted in smaller, flatter tissue clumps with many concentrated, though unhealthy, cells **(Fig. 47A)**. The digestive solution seemed to reduce the amount of scale shards, fibrous particles, and other common but unwanted debris, resulting in a cleaner sample. However, the chemicals had an adverse effect on the keratocytes; they did not adhere and flatten to the coverslip, but instead remained round and detached **(Fig. 47C)**. Mechanical manipulation by itself did not cause cellular trauma like the chemical manipulation did. The control, non-digested cell clumps that had merely been pipetted and shaken vigorously in culture media, appeared to be much more adherent and motile **(Fig. 47D).**

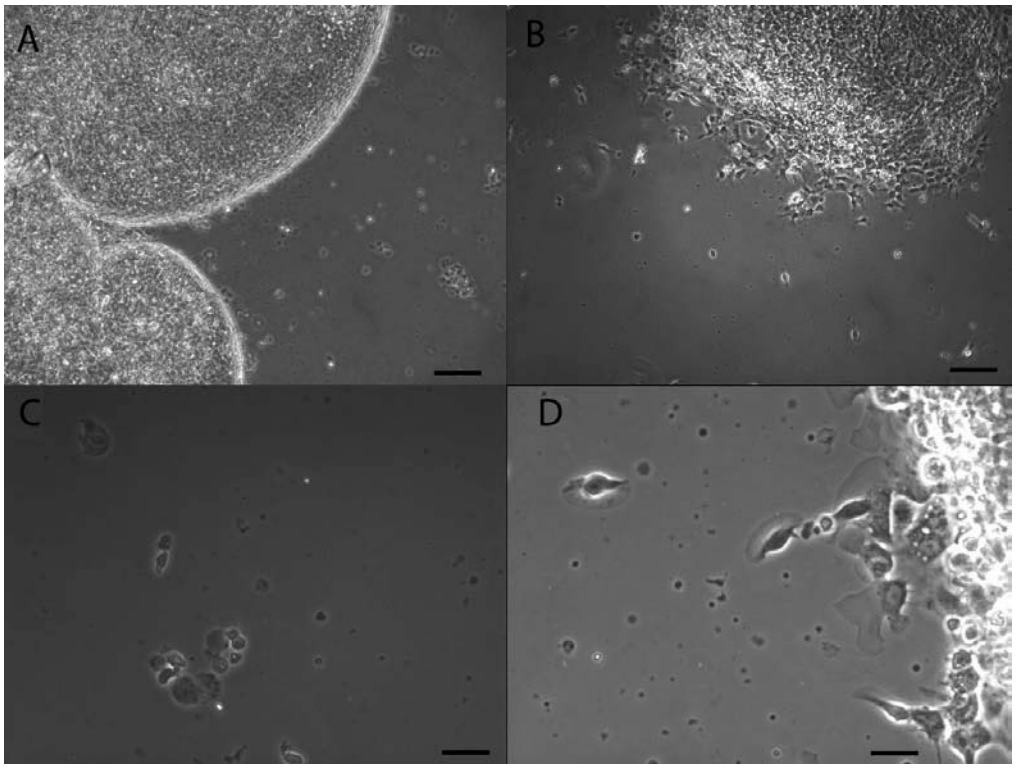

Figure 47. Keratocyte clumps in digested and undigested preparations.

There are many cells present in and around the digested tissue (panel A), but they do not look the same as those in the undigested tissue (panel B), even under 100x magnification. The cells in panel B appear healthier, more adherent, and more motile. At 400x this is even more apparent (panels C and D). Healthy cells in panel D have formed or are starting to form the characteristic crawling keratocyte morphology, while those in panel C are round and probably non-adherent. Scale bar = 40 µm (A,B) and 10 µm (C,D).

Future research: promises, problems, and questions

One branch of biology where motility experiments hold much promise is stem cell biology. Adult mesenchymal stem cell motility in vitro is not well-characterized in literature, which tends to focus mainly on their ability to differentiate. For instance, data on the crawling velocity of mammalian mesenchymal stem cells seems to be obscure or non-existent. Most research pertaining to their migratory abilities is involved in stem cell transplantation, and subsequent homing behavior in situ following engraftment. A time-lapse experiment performed on cells induced to migrate into a wounded area of the monolayer would be useful to establish an approximate migration velocity for mesenchymal stem cells.

A related study concerns the NPC1 mutation briefly mentioned previously **(Fig. 34)**. The murine model of Niemann-Pick Disease Type C (a devastating and fatal recessive genetic disease in humans) has brittle bone structure, stunted growth, and chronic joint inflammation in addition to some of the human symptoms, which include muscular weakening and Parkinsons-like ataxia. The disease is caused by a mutation in either the NPC1 or NPC2 gene, which encode proteins that work together to traffic intracellular cholesterol out of the late endosome (LE) and, ultimately, out of the cell (Subramanian & Balch 2008). Build-up of endogenous cholesterol occurs when one of these proteins is absent or abnormally formed, and has terrible consequences for the affected individual.

Mice with a recessive mutation on the NPC1 gene (phenotypically

characterized by a reduced cholesterol trafficking ability) have adult mesenchymal stem cells (MSCs) with distinct morphological differences from wild type stem cells. They have smaller lamellipodia, and they have more filopodia than wild type stem cells. Compact bone and bone-marrow derived MSCs of NPC1 mice also may have a reduced functionality, which could be partially investigated by evaluating their migration into scored areas of the coverslip under time-lapse microscopy. Further experimentation could be done by treating NPC1 mouse stem cells with cyclodextrins, which are known to alleviate the build-up of endolysosomal cholesterol. Another treatment could involve exogenous cholesterol, which would most likely have an adverse effect on motility because it would contribute even more to the high level of cholesterol build-up conferred by the disease. This could be shown by reduced lamellipodia formation, increased filopodia size and quantity, and slower cell migration under time lapse. Since it is evident that migration is a key property of bone marrow derived mesenchymal stem cells, a study of this sort could demonstrate if and why such drastic physiological disruption occurs when MSCs are unable to move to a target area.

All experiments conducted during the course of this investigation involved cultured cells. Coverslips are artificial substrates, so cell crawling may look and function differently in the cell's natural environment. The three-dimensional niche that the cell occupies in the body has many different components that provide information to the cell and affect its behavior. Signal molecules, chemical

gradients, and variable substrate composition are all found in the environment of the tissue. To reproduce in vitro the exact conditions under which the cell is naturally found would be impossible. Therefore, any data collected from cells moving across a flat, glass coverslip – such as crawling velocity or spreading area – are data collected in an artificial environment and may not truly characterize cells in vivo.

However, as previously discussed, in vitro motility studies continue to be extremely useful. In many experiments, behavioral differences that may arise in vitro versus in vivo are not relevant to the investigation, making data collected from cultured cells perfectly valid.

The promise and potential of cell migration microscopy is certainly being realized. Researchers at the helm of powerful imaging equipment can see structures that are intricate beyond imagination. Technological innovations have revolutionized microscopy, but in the process have created their own, autocatalytic reaction. The more a scientist sees of the natural world that exists inside the cell, the more she realizes she can't see, and the more questions she asks. Some might argue that science has discovered and characterized almost everything there is to know about cell motility, at least in terms of its structures and morphology; however, microscopy continues to be an indispensible tool of the biologist's trade. It will address a great deal of the questions still waiting to be answered.

REFERENCES

Abercrombie, M., J. Heaysman, and S. Pegrum. 1970. The locomotion of fibroblasts in culture III: movements of particles on the dorsal surface of the leading lamella. *Experimental Cell Research* 62: 389-398.

Abraham, V., V. Krishnamurthi, D. Taylor, and F. Lanni. 1999. The actin-based nanomachine at the leading edge of migrating cells. *Biophysical Journal* 77: 1721-1732.

Alexandrova, A., K. Arnold, S. Schaub, J. Vasiliev, J. Meister, A. Bershadsky, and A. Verkhovsky. 2008. Comparative dynamics of retrograde actin flow and focal adhesions: formation of nascent adhesions triggers transition from fast to slow flow. *PLoS ONE* 3(9): e3234.

Ananthakrishnan, R. and A. Ehrlicher. 2007. The forces behind cell movement. *Inernational Journal of Biological Sciences* 3(5): 303-317.

Bailly, M. And J. Condeelis. 2002. Cell motility: insights from the backstage. *Nature Cell Biology* 4: e292-e294.

Bajénoff, M., J. Egen, L. Koo, J. Laugier, F. Brau, N. Glaichenhaus, and R. Germain. 2006. Stromal cell networks regulate lymphocyte entry, migration, and territoriality in lymph nodes. *Immunity* 25: 989-1001.

Bauer, A., T. Jackson, and Y. Jiang. 2007. A cell-based model exhibiting branching and anastomosis during tumor-induced angiogenesis. *Biophysical Journal* 92: 3105-3121.

Bonner, J.T. 1947. Evidence for the formation of cell aggregates by chemotaxis in the development of the slime mold *Dictyostelium discoideum*. *Journal of Experimental Zoology* 106: 1-26.

Borm, B., R. Requardt, V. Herzog, and G. Kirfel. 2005. Membrane ruffles in cell migration: indicators of inefficient lamellipodia adhesion and compartments of actin filament reorganization. *Experimental Cell Research* 302: 83-59.

Bray, Dennis. Cell Movements From Molecules to Motility, 2nd ed. Garland Publishing: New York, 2001.

Burton, K., J. Park, and D. Taylor. 1999. Keratocytes generate traction forces in two phases. *Molecular Biology of the Cell* 10: 3745-3769.

Casanova, J.E. 2002. epithelial cell cytoskeleton and intracellular trafficking: V. confluence of membrane trafficking and motility in epithelial cell models. *American Journal of Physiology – Gastrointestinal Liver Physiology* 283(5): 1015-1019.

Chakravarti, R., V. Sapountzi, and J.C. Adams. 2005. Functional role of syndecan-1 cytoplasmic V region in lamellipodial spreading, actin bundling, and cell migration. *Molecular Biology of the Cell* 16(8): 3678-3691.

Chowdhury, F., N. Sungsoo, D. Li, Y. Poh, T. Tanaka, F. Wang, and N. Wang. 2010. Cell material property dictates stress-induced spreading and differentiation in embryonic stem cells. *Nature Materials* 9(1): 82-88.

Friedl, P. S. Borgmann, and E. Bröcker. 2001. Amoeboid leukocyte crawling through extracellular matrix: lessons from the *Dictyostelium* paradigm of cell movement. *Journal of Leukocyte Biology* 70: 491-509.

Goley, E. and M. Welch. 2006. The Arp2/3 complex: an actin nucleator comes of age. *Nature Reviews Molecular Cell Biology* 7: 713-726.

Konijn, T., D. Barkley, Y. Chang, and J.T. Bonner. 1968. Cyclic AMP: A naturally occurring acrasin in the cellular slime molds. *The American Naturalist* 102(925): 225-233.

Lo, C., H. Wang, M. Dembo, and Y. Wang. 2000. Cell movement is guided by the rigidity of the substrate. *Biophysical Journal* 79(1): 144-152.

Mejillano, M., S. Kojima, D. Applewhite, F. Gertler, T. Svitkina, and G. Borisy. 2004. Lamellipodial versus filopodial mode of the actin nanomachinery: pivotal role of the filament barbed end. *Cell* 118(3): 363-373.

Mitchison, T. and L. Cramer. 1996. Actin-based cell motility and cell locomotion. *Cell* 84: 371-379.

O'Neill, G. 2009. The coordination between actin filaments and adhesion in mesenchymal migration. *Cell Adhesion and Migration* 3(4): 355-357.

Robenek, H. and N. Severs. 2008. Recent advances in freeze-fracture electron

microscopy: the replica immunolabeling technique. *Biological Procedures Online* 10(1): 9-19.

Ronot, X., A. Doisy, and P. Tracqui. 2000. Quantitative study of dynamic behavior of cell monolayers during in vitro wound healing by optical flow analysis. *Cytometry* 41: 19-30.

Rørth, P. 2009. Collective Cell Migration. *Annual Review of Cell and Developmental Biology* 25(1): 407-429.

Sammak, P., L. Hinman, P. Tran, M. Sjaastad, and T. Machen. 1997. How do injured cells communicate with the surviving cell monolayer? *Journal of Cell Science* 110: 465-475.

Seluanov, A., C. Hine, J. Azpurua, M. Feigenson, M. Bozzella, Z. Mao, K. Catania, and V. Gorbunova. 2009. Hypersensitivity to contact inhibition provides a clue to cancer resistance of naked mole-rat. *Proceedings of the National Academy of Sciences* 106(46): 19352-19357.

Shroff, H., H. White, and E. Betzig. 2008. Photoactivated localization microscopy (PALM) of adhesion complexes. *Current Protocols in Cell Biology* 41: 4.21.1-4.21.27.

Shtengel, G., J. Galbraith, C. Galbraith, J. Lippincott-Schwartz, J. Gillette, S. Manley, R. Sougrat, C. Waterman, P. Kanchanawong, M. Davidson, R. Fetter, and H. Hess. 2009. Interferometric fluorescent super-resolution microscopy resolves 3D cellular ultrastructure. *Proceedings of the National Academy of Sciences* 106(9): 3125-3130.

Singer, A. and R. Clark. 1999. Cutaneous wound healing. *The New England Journal of Medicine* 341(10): 738-746.

Skloot, Rebecca. The Immortal Life of Henrietta Lacks. Crown Publishers, New York: 2010.

Subramanian, K., & Balch, W. E. (2008). NPC1/NPC2 function as a tag team duo to mobilize cholesterol. *Proceedings of the National Academy of Sciences* 105(40): 15223-15224.

Svitkina, T. 2007. Electron microscopic analysis of the leading edge in migrating cells. *Methods in Cell Biology* 79: 295-319.

Theriot, J. 2000. The polymerization motor. *Traffic* 1: 19-28.

Tountas, N. and D. Brautigan. 2004. Migration and retraction of endothelial and epithelial cells require PHI-1, a specific protein-phosphatase-1 inhibitor protein. *Journal of Cell Science* 117: 5905-5912.

Vasanji, A., P. Ghosh, L. Graham, S. Eppell, and P. Fox. 2004. Polarization of plasma membrane microviscosity during endothelial cell migration. *Developmental Cell* 6(1): 29-41.

Wilson, C., M. Tsuchida, G. Allen, E. Barnhart, K. Applegate, P. Yam, L. Ji, K. Keren, G. Danuser, and J. Theriot. 2010. Myosin II contributes to cell-scale actin network treadmilling through network disassembly. *Nature* 465: 373-379.

Yang C., L. Czech, S. Gerboth, S. Kojima, G. Scita, and T. Svitkina. 2007. Novel roles of formin mDia2 in lamellipodia and filopodia formation in motile cells. *PLoS Biology* 5(11): e317.

Yang C., M. Hoelzle, A. Disanza, G. Scita, and T. Svitkina. 2009. Coordination of membrane and actin cytoskeleton dynamics during filopodia protrusion. *PLoS ONE* 4(5): e5678.